LED Selection and Orientation and Power Adaptation for Visible Light Positioning Systems

Baran Asilioglu, *Student Member, IEEE*, and Sinan Gezici, *Fellow, IEEE*

***Abstract*—We investigate a visible light positioning (VLP) system in which a number of light emitting diode (LED) transmitters emit signals over a certain number of time intervals for localizing a visible light communication (VLC) receiver. We formulate the problem of LED selection and orientation adaptation, with the aim of optimally determining the LED transmitter and its orientation vector to be employed in each time interval for minimizing the average Cramér-Rao lower bound (CRLB) on position estimation. Due to the complexity of the proposed problem, we take a discretization approach in which the orientation vector of each LED transmitter is confined to a finite set as in digital implementations. Then, we obtain a convex problem via relaxation and propose a solution approach based on the relaxed solution and a swap algorithm. We also formulate the problem of joint LED selection, orientation adaptation, and power allocation. For this problem, we extend the discretization approach by generating a power vector corresponding to each LED orientation. Then, we develop a new formulation over all the design parameters via relaxation, and propose a low-complexity algorithm using that formulation and a swap algorithm. We present numerical examples to illustrate the effectiveness of the proposed approaches. In particular, it is shown that, in some cases, instead of employing multiple LEDs over a number of time intervals, using the same LED with different orientations can be more desirable for accurate localization. Moreover, the proposed joint optimization approach can notably reduce the average CRLB compared to the uniform power allocation approach.**

***Index Terms*—Light emitting diode, visible light positioning, estimation, Cramér-Rao lower bound.**

I. Introduction

VISIBLE light communication (VLC) is considered to be one of the key technologies for 6G wireless networks [2], [3]. In addition to providing high speed data transmission, visible light systems can also provide accurate position information based on low-cost received power measurements, making them well-suited for indoor localization applications [4], [5]. Unlike radio frequency (RF) based localization systems, visible light positioning (VLP) systems do not suffer from bandwidth limitations and interference from RF communications. Hence, they provide an effective alternative to RF based systems in various indoor localization scenarios by utilizing existing infrastructures with low additional costs [4], [6].

In the literature, a multitude of position estimation algorithms are proposed for VLP systems based on various parameter types such as received signal strength (RSS) [7], [8], [9], [10], [11], [12], time of arrival (TOA) [13], [14], angle of arrival (AOA) [15], [16], and time-difference-of-arrival (TDOA) [17]. In addition, combinations of multiple parameters are also analyzed [18], [19], [20]. In [20], both the RSS and AOA parameters are utilized in a multiple-input single-output system for three-dimensional (3D) localization and the Cramér-Rao lower bound (CRLB) is derived using the RSS information. In practical systems, RSS measurements are widely used in designs of VLP systems as they facilitate cost-effective hardware implementation accompanied with sufficiently high accuracy [4], [6]. Therefore, RSS based VLP is preferable over TOA based approaches to avoid synchronization and time delay estimation complexity [8]. Learning-based methods are also employed for VLP systems as in [21], [22], [23], [24], and [25]. Common VLP systems in the literature use fixed LED orientations during the localization process. However, with the advancement of technology, it is possible to mechanically adapt the orientation of an LED transmitter or to use an intelligent reflecting surface (IRS) at the transmitter to effectively steer the beam [26]. In [27], it is noted that the use of one LED transmitter with different orientations can lead to accurate positioning. In [28], an RSS based system with multiple LEDs located at a fixed point with different orientations is used for 3D localization of a VLC receiver. In [29], the authors introduce a movable access point (AP) aided architecture for integrated visible-light communication and sensing (IVLCS), by allowing LED APs to reposition dynamically, effectively addressing the LED placement problem through selection of optimal AP locations. However, that work assumes fixed LED orientations, and restricts each LED to a single activation at its assigned position, leaving the potential gains from adaptive orientation control and multiple usage of LEDs unexplored. In [30], orientation vectors of LED transmitters are optimized in order to provide uniform illumination in an indoor environment. In [31], the impact of the tilts of LEDs on positioning performance is investigated for certain tilt angles, and it is shown that positioning accuracy can be improved via tilted LEDs. However, a generic problem of developing an adaptation strategy is not considered. In [32], LED tilt and gain are estimated with offline training to perform 2D localization for a specific case considering a Lambertian

Received 29 April 2025; revised 27 August 2025 and 22 September 2025; accepted 27 September 2025. Date of publication 7 October 2025; date of current version 23 December 2025. An earlier version of this paper was presented in part at the 2025 IEEE International Symposium on Personal, Indoor and Mobile Radio Communications (PIMRC) [1]. The associate editor coordinating the review of this article and approving it for publication was A. M. Vegni. *(Corresponding author: Sinan Gezici.)*

The authors are with the Department of Electrical and Electronics Engineering, Bilkent University, 06800 Ankara, Türkiye (e-mail: baran.asilioglu@bilkent.edu.tr; gezici@ee.bilkent.edu.tr).

Digital Object Identifier 10.1109/TCOMM.2025.3618677

order of unity. That work also illustrates the effects of LED tilts on positioning performance; however, it does not focus on LED selection or orientation adaptation.

Although the effects of LED orientations on positioning accuracy and illumination are considered in the literature (e.g., [26], [27], [28], [29], [30], [31], [32]), there is no work that investigates how to optimally choose LED transmitters and determine their optimal orientation vectors during the localization process in order to achieve the best localization accuracy in VLP systems. (Due to the unique propagation characteristics of visible light signals [4], LED orientation adaptation differs notably from beamforming in RF systems.) Existing related methods summarized in the previous paragraph illustrate the significant effects of LED orientations on localization accuracy. However, an orientation adaptation and selection strategy for LED transmitters for optimizing localization performance in a VLP system is not available in the literature. Moreover, the problem of jointly optimizing LED orientations and powers has not been considered previously.

In this manuscript, we investigate an indoor VLP system with multiple LED transmitters, which emit signals over a certain number of time intervals to localize a VLC receiver. We formulate the problem of LED selection and orientation vector optimization with the aim of determining which LED transmitter to employ in each time interval together with its optimal orientation vector by considering the minimization of the average CRLB on position estimation for a set of possible receiver positions. Considering digital implementations, we confine the orientation vectors of LED transmitters to finite sets, and then use a convex relaxation approach and a swap algorithm to develop a technique for LED selection and orientation adaptation. We also formulate the problem of joint LED selection, orientation adaptation, and power allocation. For this problem, we extend the discretization approach by generating a power vector corresponding to each LED orientation. Moreover, we present a generic and low-complexity joint optimization algorithm to optimize power allocation and LED selection and orientation adaptation. We show the effectiveness of the proposed approaches via simulations by presenting comparisons with conventional approaches. The main contributions and novelty of this work are as follows:

- A new problem formulation is presented for optimally determining LED transmitters and their orientation vectors to be employed over a certain number of time intervals during the localization of a VLC receiver by considering the average CRLB metric.
- By confining the LED orientation vectors to finite sets (as in digital implementations), a convex optimization problem is obtained via relaxation. Then, a low-complexity solution approach based on the relaxed solution and a swap algorithm is proposed.
- It is shown that, over a number of time intervals, using the same LED with different orientation vectors can be preferable in some cases over the use of multiple LED transmitters.
- The proposed approach is extended to obtain a new optimization problem for joint LED selection and *power* and orientation adaptation by assigning a power element for each possible LED orientation. The new problem is solved via relaxation and a swap algorithm.
- It is shown via simulations that jointly optimizing the powers and orientation vectors of LED transmitters can significantly improve the localization performance of practical maximum likelihood (ML) estimators.

In the conference version of this study [1], we present the LED selection and orientation adaptation strategy, Algorithm 1, in Section III. In this manuscript, we also provide the following extensions: (i) Joint optimization of LED selection and orientation and power adaptation is proposed. (ii) A new optimization problem is obtained for the proposed problem, and a low-complexity algorithm (Algorithm 2) is presented to solve it in a close-to-optimal manner. (iii) Extensive simulations are conducted to investigate the performance of the proposed approaches in Section VI. (iv) Extensions are presented to incorporate illumination constraints into the proposed formulations and to investigate the case of multiple VLC receivers.

As an approach related to LED orientation adaptation, orientation vectors of photo-detectors at VLC receivers can also be adjusted to improve localization and communication performance of visible light systems [33], [34], [35], [36], [37], [38]. For example, in [33] and [34], a VLP system is realized by utilizing a single LED transmitter with a fixed orientation and a VLC receiver with a single rotatable photo-detector. Then, position estimation can be performed based on received power measurements collected by the photo-detector at different locations in the environment by rotating it multiple times [34]. The idea of adjustable orientation vectors is employed in angle diversity receivers (ADRs) to improve performance of VLC systems as in [37], [38], and [39]. For instance, an ADR structure is proposed in [39] to reduce the signal-to-interference-plus-noise ratio (SINR) fluctuations in multi-cell VLC systems, where one top photo-detector and multiple inclined side photo-detectors are used. By optimizing the inclination angle of the side photo-detectors, the SINR fluctuation is minimized over a certain receiving plane. Although orientations of photo-detectors are optimized subject to certain geometric constraints in the literature such as [34] and [39], a generic optimal design of photo-detector orientations has not been considered in the literature. The idea of LED selection and orientation adaptation via discretization and convex relaxation approach proposed in this manuscript can also be applied to the orientation adaptation of photo-detectors at VLC receivers (Remark 5).

The rest of this manuscript is organized as follows: Section II describes the system model and problem formulation. Section III presents the CRLB derivations and the proposed orientation adaptation strategy. Section IV deals with a special case of the proposed formulation for comparison purposes. In Section V, the problem formulation and the proposed algorithm for the joint optimization of LED selection and power and orientation adaptation are given. The simulation results are presented in Section VI. Extensions related to consideration of illumination constraints and multiple VLC receivers are investigated in Section VII, and concluding remarks are made in Section VIII.

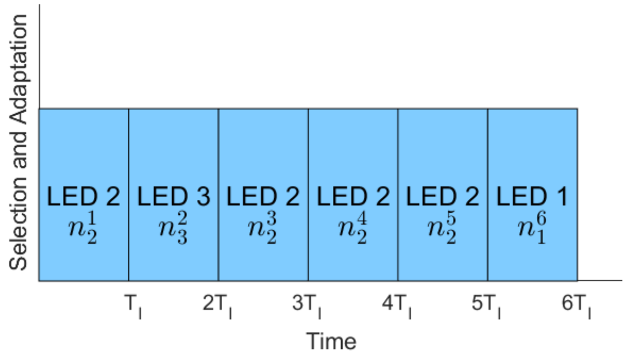

Fig. 1. An example of LED selection and orientation adaptation over $N_{\rm I} = 6$ time intervals of duration T_I, using $N_{\rm L} = 4$ LED transmitters, where the indices of the selected LED transmitters are given by $s(1) = 2$, $s(2) = 3$, $s(3) = 2$, $s(4) = 2$, $s(5) = 2$, and $s(6) = 1$. As will be illustrated in Section VI, it may be optimal not to employ all the LEDs (such as LED 4 in this example) during the localization process.

II. System Model and Problem Formulation

We consider an indoor VLP system with $N_{\rm L}$ LED transmitters at known locations denoted by $\boldsymbol{l}_1, \ldots, \boldsymbol{l}_{N_{\rm L}}$ in the 3D space. The orientation vectors of the LED transmitters are adjustable for the purpose of improving the localization performance of a VLC receiver, which estimates its own position based on signals collected from the LED transmitters.

As the position of a VLC receiver is not known during the localization process, we consider prior statistical knowledge about the position of the VLC receiver. In particular, it is assumed that the VLC receiver can be at position $\boldsymbol{x}_k$ with probability w_k for $k = 1, \ldots, N_{\rm U}$, where $N_{\rm U}$ denotes the number of possible positions for the VLC receiver, $w_k \geq 0 \forall k$, and $\sum_{k=1}^{N_{\rm U}} w_k = 1$. In addition, it is assumed that the VLC receiver knows its orientation vector, e.g., via a gyroscope [13], at each possible position. In particular, $\bar{\boldsymbol{n}}_k$ denotes the orientation vector of the VLC receiver at position $\boldsymbol{x}_k$ for $k = 1, \ldots, N_{\rm U}$.[1] For example, if the aim is the localization of a robot in a given environment, where the robot has a VLC receiver with a fixed orientation vector, then $\bar{\boldsymbol{n}}_k$'s are the same for all possible positions of the robot in the environment.[2]

We consider a time division multiplexing scheme such that only one LED transmitter emits signals in a given time interval [40], [41].[3] In order to provide a generic formulation, we consider localization over $N_{\rm I}$ time intervals, where one of the LED transmitters can transmit with a certain orientation vector in each interval. In this formulation, an LED transmitter is allowed to transmit in multiple time intervals with desired orientation vectors. The aim is to determine the LED transmitter and its orientation vector to be employed in each of the $N_{\rm I}$ time intervals allocated for the localization process. To this aim, we use the average CRLB as the localization accuracy metric since (i) it provides a lower bound on mean-squared errors (MSEs) of unbiased estimators, (ii) it does not rely on a specific estimator structure, and (iii) the MSE of the ML estimator converges to it asymptotically [42]. Accordingly, we propose the following optimization problem:

$$\underset{\left\{s(i), \boldsymbol{n}^i_{s(i)}\right\}_{i=1}^{N_{\rm I}}}{\text{minimize}} \quad \sum_{k=1}^{N_{\rm U}} w_k \text{CRLB}_k \left(\left\{ s(i), \boldsymbol{n}^i_{s(i)} \right\}_{i=1}^{N_{\rm I}} \right) \tag{1}$$

$$\text{subject to} \quad s(i) \in \{1, \ldots, N_{\rm L}\}, \; i = 1, \ldots, N_{\rm I} \tag{2}$$

$$\left\| \boldsymbol{n}^i_{s(i)} \right\| = 1, \; i = 1, \ldots, N_{\rm I} \tag{3}$$

where $s(i)$ specifies the index of the LED transmitter selected for the ith time interval, $\boldsymbol{n}^i_{s(i)}$ denotes the orientation vector of the $s(i)$th LED transmitter during the ith time interval, and $\text{CRLB}_k \left(\left\{ s(i), \boldsymbol{n}^i_{s(i)} \right\}_{i=1}^{N_{\rm I}} \right)$ denotes the CRLB when the VLC receiver is at position $\boldsymbol{x}_k$ and the selected LED transmitters and their orientation vectors over the $N_{\rm I}$ time intervals are specified by $\left\{ s(i), \boldsymbol{n}^i_{s(i)} \right\}_{i=1}^{N_{\rm I}}$. In Fig. 1, an example illustration is presented for LED selection and orientation adaptation for $N_{\rm I} = 6$ and $N_{\rm L} = 4$. In the next section, the CRLB expression in (1) is specified and the proposed problem in (1)–(3) is investigated.

III. LED Selection and Orientation Adaptation

We focus on the proposed formulation in (1)–(3), and provide explicit expressions for the CRLB terms in (1). Considering an asynchronous VLP system [13], [43], the VLC receiver performs localization based on received power measurements due to signals transmitted over the $N_{\rm I}$ time intervals. Let $P^{\rm RX}_{i,j,k}(\boldsymbol{x}_k, \boldsymbol{n}^i_j)$ denote the received power measurement when the VLC receiver is at position $\boldsymbol{x}_k$ based on the signal emitted in the ith time interval by the jth LED transmitter with orientation vector $\boldsymbol{n}^i_j$. Then, $P^{\rm RX}_{i,j,k}(\boldsymbol{x}_k, \boldsymbol{n}^i_j)$ can be expressed as [43], [44], [45], and [46]

$$P^{\rm RX}_{i,j,k}(\boldsymbol{x}_k, \boldsymbol{n}^i_j) = \sqrt{P^{\rm TX}_j} \tilde{H}^{\rm LOS}_{j,k}(\boldsymbol{x}_k, \boldsymbol{n}^i_j) + \xi_{i,j,k} \tag{4}$$

for $i = 1, \ldots, N_{\rm I}$, where $j \in \{1, \ldots, N_{\rm L}\}$ and $k \in \{1, \ldots, N_{\rm U}\}$. In (4), $P^{\rm TX}_j$ is the transmit power parameter of the jth LED transmitter (the square-root is used to simplify the analysis in Section V), $\tilde{H}^{\rm LOS}_{j,k}(\boldsymbol{x}_k, \boldsymbol{n}^i_j)$ is the channel coefficient of the LOS path between the jth LED transmitter with orientation vector $\boldsymbol{n}^i_j$ and the VLC receiver at position $\boldsymbol{x}_k$,[4] and $\xi_{i,j,k}$ is a zero-mean Gaussian noise component with a variance of σ^2, which is independent of $\xi_{\tilde{i},\tilde{j},\tilde{k}}$ for all $\tilde{i} \neq i$ and $\tilde{j} \neq j$ [45].[5]

[1] If there are multiple possible orientations of the VLC receiver at a given position, this can be incorporated into the formulation by repeating the same position multiple times with different orientations.

[2] Although the number of possible positions is taken to be finite for simplicity, the results can be extended to infinite number of possible positions by devising a prior probability density function.

[3] Considering low mobilities in indoor VLP systems, it is assumed that the position of the VLC receiver does not change during the localization process.

[4] We consider a LOS channel model and omit multipath effects as in [7], [8], [13], [47], and [48] due to the following reasons: (i) LOS components are significantly stronger than multipath components in visible light system [4]. (ii) When LOS LEDs exist, using them multiple times with various orientations can be more beneficial than using non-LOS LEDs during LED selection and orientation adaptation; hence, non-LOS LEDs may not be utilized for localization. (iii) Taking into account the multipath components makes the received signal model very complicated, preventing the theoretical analysis of the LED selection and orientation adaptation problem, which is studied for the first time in this manuscript.

[5] Independence of $\xi_{i,j,k}$'s for different k indices is irrelevant as the CRLB is calculated for each k (i.e., each possible position of the VLC receiver) separately.

The channel coefficients in (4) can be calculated as [49]:

$$\tilde{H}^{\rm LOS}_{j,k}(\boldsymbol{x}_k,\boldsymbol{n}^i_j)=H^{\rm LOS}_{j,k}(\boldsymbol{x}_k,\boldsymbol{n}^i_j)\mathbb{1}_{\{(\boldsymbol{x}_k-\boldsymbol{l}_j)^T\boldsymbol{n}^i_j>0,\,(\boldsymbol{l}_j-\boldsymbol{x}_k)^T\bar{\boldsymbol{n}}_k>0\}} \tag{5}$$

with

$$H^{\rm LOS}_{j,k}(\boldsymbol{x}_k,\boldsymbol{n}^i_j)=\frac{(m_j+1)A\left((\boldsymbol{x}_k-\boldsymbol{l}_j)^T\boldsymbol{n}^i_j\right)^{m_j}(\boldsymbol{l}_j-\boldsymbol{x}_k)^T\bar{\boldsymbol{n}}_k}{2\pi\|\boldsymbol{x}_k-\boldsymbol{l}_j\|^{m_j+3}} \tag{6}$$

where m_j is the Lambertian order for the jth LED transmitter, and A is the area of the photo-detector at the VLC receiver. In (5), the indicator function $\mathbb{1}_{\{\cdot\}}$ specifies whether the jth LED transmitter having an orientation vector $\boldsymbol{n}^i_j$ can communicate with the VLC receiver at position $\boldsymbol{x}_k$ having an orientation vector of $\bar{\boldsymbol{n}}_k$. In particular, considering the use of a hemispherical lens at the VLC receiver, the field-of-view of the photo-detector at the VLC receiver is taken to be 90° [50], [51]. Therefore, it is assumed that as long as the LOS path between the jth LED transmitter and the VLC receiver at position $\boldsymbol{x}_k$ forms acute angles with the orientation vectors $\bar{\boldsymbol{n}}_k$ and $\boldsymbol{n}^i_j$, there exists a connection between the jth LED transmitter with orientation vector $\boldsymbol{n}^i_j$ and the VLC receiver with orientation vector $\bar{\boldsymbol{n}}_k$ (as specified by the inequalities in the indicator function in (5)).

The VLP system described above is asynchronous since the VLC receiver does not have clock synchronization with the LED transmitters. Therefore, while estimating its own position, the VLC receiver cannot utilize the time delay information, and measures the received powers of the signals sent from the LED transmitters for localization purposes. On the other hand, the LED transmitters are controlled by a central localization unit which controls the selection and orientation adaptation of the LED transmitters. This localization unit makes sure that one LED transmitter with desired parameters performs transmission during each time interval; hence, time division multiplexing is realized in this manner. At the beginning of each transmission interval, pilot signals are sent by the LED transmitters, which are used by the VLC receiver for synchronizing with the time intervals and determining the parameters of the LED transmitters.

Consider a strategy of LED selection and orientation adaptation specified by $\{s(i),\boldsymbol{n}^i_{s(i)}\}_{i=1}^{N_{\rm I}}$ as in (1). For that given strategy, the following received power measurements are obtained for the VLC receiver position $\boldsymbol{x}_k$: $\left\{P^{\rm RX}_{i,s(i),k}(\boldsymbol{x}_k,\boldsymbol{n}^i_{s(i)})\right\}_{i=1}^{N_{\rm I}}$ based on the description in (4). We represent the vector of measurements related to position $\boldsymbol{x}_k$ for the strategy specified by $\{s(i),\boldsymbol{n}^i_{s(i)}\}_{i=1}^{N_{\rm I}}$ as $\boldsymbol{P}^{\rm RX}_k(\{s(i),\boldsymbol{n}^i_{s(i)}\}_{i=1}^{N_{\rm I}})$, that is,

$$\boldsymbol{P}^{\rm RX}_k\left(\{s(i),\boldsymbol{n}^i_{s(i)}\}_{i=1}^{N_{\rm I}}\right)\triangleq\big[P^{\rm RX}_{1,s(1),k}(\boldsymbol{x}_k,\boldsymbol{n}^1_{s(1)}),\\ P^{\rm RX}_{2,s(2),k}(\boldsymbol{x}_k,\boldsymbol{n}^2_{s(2)}),\ldots,P^{\rm RX}_{N_{\rm I},s(N_{\rm I}),k}(\boldsymbol{x}_k,\boldsymbol{n}^{N_{\rm I}}_{s(N_{\rm I})})\big]. \tag{7}$$

Then, the log-likelihood function for estimating the position parameter $\boldsymbol{x}_k$ based on the power measurements given by $\boldsymbol{P}^{\rm RX}_k\left(\{s(i),\boldsymbol{n}^i_{s(i)}\}_{i=1}^{N_{\rm I}}\right)$ in (7) can be obtained via (4) as

$$\log p\left(\boldsymbol{P}^{\rm RX}_k\left(\{s(i),\boldsymbol{n}^i_{s(i)}\}_{i=1}^{N_{\rm I}}\right)\Big|\boldsymbol{x}_k\right)=\tilde{\kappa}-\frac{1}{2\sigma^2}\times\\ \sum_{i=1}^{N_{\rm I}}\left(P^{\rm RX}_{i,s(i),k}(\boldsymbol{x}_k,\boldsymbol{n}^i_{s(i)})-\sqrt{P^{\rm TX}_{s(i)}}\tilde{H}^{\rm LOS}_{s(i),k}(\boldsymbol{x}_k,\boldsymbol{n}^i_{s(i)})\right)^2 \tag{8}$$

where $\tilde{\kappa}$ is a constant independent of $\boldsymbol{x}_k$. The ML estimator for the parameter $\boldsymbol{x}_k$, which is the maximizer of the log-likelihood function in (8), can be obtained as follows:

$$\hat{\boldsymbol{x}}_{k,\rm ML}=\arg\min_{\boldsymbol{x}_k\in\mathcal{S}}\sum_{i=1}^{N_{\rm I}}\Big(P^{\rm RX}_{i,s(i),k}(\boldsymbol{x}_k,\boldsymbol{n}^i_{s(i)})\\ -\sqrt{P^{\rm TX}_{s(i)}}\tilde{H}^{\rm LOS}_{s(i),k}(\boldsymbol{x}_k,\boldsymbol{n}^i_{s(i)})\Big)^2 \tag{9}$$

where $\mathcal{S}$ denotes the set of possible locations for the VLC receiver.

Let $\mathbf{I}_k\left(\{s(i),\boldsymbol{n}^i_{s(i)}\}_{i=1}^{N_{\rm I}}\right)$ denote the Fisher information matrix (FIM) related to the estimation of $\boldsymbol{x}_k$ based on the power measurements $\boldsymbol{P}^{\rm RX}_k\left(\{s(i),\boldsymbol{n}^i_{s(i)}\}_{i=1}^{N_{\rm I}}\right)$ given by (7). Similarly to [13] and [46], this FIM can be derived from (8) as

$$\left[\mathbf{I}_k\left(\{s(i),\boldsymbol{n}^i_{s(i)}\}_{i=1}^{N_{\rm I}}\right)\right]_{t_1,t_2}\\ =\sum_{i=1}^{N_{\rm I}}\frac{P^{\rm TX}_{s(i)}}{\sigma^2}\frac{\partial H^{\rm LOS}_{s(i),k}(\boldsymbol{x}_k,\boldsymbol{n}^i_{s(i)})}{\partial x_{k,t_1}}\\ \times\frac{\partial H^{\rm LOS}_{s(i),k}(\boldsymbol{x}_k,\boldsymbol{n}^i_{s(i)})}{\partial x_{k,t_2}}\mathbb{1}_{\left\{(\boldsymbol{x}_k-\boldsymbol{l}_{s(i)})^T\boldsymbol{n}^i_{s(i)}>0,\,(\boldsymbol{l}_{s(i)}-\boldsymbol{x}_k)^T\bar{\boldsymbol{n}}_k>0\right\}} \tag{10}$$

for $t_1,t_2\in\{1,2,3\}$, where the indicator function is used to specify whether the $s(i)$th LED transmitter can communicate with the VLC receiver when it is at position $\boldsymbol{x}_k$, $H^{\rm LOS}_{s(i),k}(\boldsymbol{x}_k,\boldsymbol{n}^i_{s(i)})$ is as defined in (6), and the derivative in (10) is expressed as [46, Eq. (13)]

$$\frac{\partial H^{\rm LOS}_{s(i),k}(\boldsymbol{x}_k,\boldsymbol{n}^i_{s(i)})}{\partial x_{k,t}}=\frac{-(m_{s(i)}+1)A}{2\pi\|\boldsymbol{x}_k-\boldsymbol{l}_{s(i)}\|^{m_{s(i)}+3}}\\ \times\Big[\bar{n}_{k,t}\left((\boldsymbol{x}_k-\boldsymbol{l}_{s(i)})^T\boldsymbol{n}^i_{s(i)}\right)^{m_{s(i)}}\\ -m_{s(i)}n^i_{s(i),t}\left((\boldsymbol{x}_k-\boldsymbol{l}_{s(i)})^T\boldsymbol{n}^i_{s(i)}\right)^{m_{s(i)}-1}(\boldsymbol{l}_{s(i)}-\boldsymbol{x}_k)^T\bar{\boldsymbol{n}}_k\\ +(m_{s(i)}+3)(x_{k,t}-l_{s(i),t})\\ \times\frac{\left((\boldsymbol{x}_k-\boldsymbol{l}_{s(i)})^T\boldsymbol{n}^i_{s(i)}\right)^{m_{s(i)}}(\boldsymbol{l}_{s(i)}-\boldsymbol{x}_k)^T\bar{\boldsymbol{n}}_k}{\|\boldsymbol{x}_k-\boldsymbol{l}_{s(i)}\|^2}\Big] \tag{11}$$

with $x_{k,t}$, $\bar{n}_{k,t}$, $n^i_{s(i),t}$, and $l_{s(i),t}$ denoting the t-th components of vectors $\boldsymbol{x}_k$, $\bar{\boldsymbol{n}}_k$, $\boldsymbol{n}^i_{s(i)}$, and $\boldsymbol{l}_{s(i)}$, respectively.

Remark 1: The elements of the FIM in (10) are not defined if $(\boldsymbol{x}_k-\boldsymbol{l}_{s(i)})^T\boldsymbol{n}^i_{s(i)}=0$ or $(\boldsymbol{l}_{s(i)}-\boldsymbol{x}_k)^T\bar{\boldsymbol{n}}_k=0$ for any i since $\tilde{H}^{\rm LOS}_{s(i),k}(\boldsymbol{x}_k,\boldsymbol{n}^i_{s(i)})$ in (8) is not differentiable with respect to $\boldsymbol{x}_k$ at such points (see (5)). However, the set of such boundary points will have zero probability if the prior distribution of the VLC receiver position corresponds to a continuous random variable in a given three-dimensional environment. Also, in practice, the estimation accuracy at such boundary points will be the same as that when the LED transmitter associated with that boundary point is not connected to the VLC receiver.□

The CRLB on the MSE of any unbiased position estimator $\widehat{\boldsymbol{x}}_k$ for the VLC receiver position $\boldsymbol{x}_k$ can be specified as [42]

$$\mathrm{E}\left\{\|\widehat{\boldsymbol{x}}_k-\boldsymbol{x}_k\|^2\right\} \geq \operatorname{trace}\left\{\mathbf{I}_k^{-1}\left(\{s(i),\boldsymbol{n}_{s(i)}^i\}_{i=1}^{N_\mathrm{I}}\right)\right\} \triangleq \mathrm{CRLB}_k\left(\left\{s(i),\boldsymbol{n}_{s(i)}^i\right\}_{i=1}^{N_\mathrm{I}}\right) \quad (12)$$

which is evaluated based on the expressions in (10) and (11).

From (10)–(12), the problem in (1)–(3), and its special case in (26)-(27), can be stated explicitly, revealing the fact that they are non-convex problems with high computational complexity. In particular, even for the special case in (26)-(27) which involves no LED transmitter selection, a search over a $2N_\mathrm{L}$-dimensional space is required. Therefore, we aim to propose an approach that can closely approximate the solution of (1)–(3) in a low-complexity manner, as described in the following.

Suppose that the orientation vectors of the LEDs can only be set to finitely many predetermined possible values. (This is a practical assumption when the orientations of the LEDs are digitally controlled.) Let

$$\mathcal{N}_j = \left\{\tilde{\boldsymbol{n}}_{j,1},\ldots,\tilde{\boldsymbol{n}}_{j,|\mathcal{N}_j|}\right\} \quad (13)$$

represent the set of possible values for the orientation vector of the jth LED transmitter for $j\in\{1,\ldots,N_\mathrm{L}\}$, where $|\mathcal{N}_j|$ denotes the number of elements in $\mathcal{N}_j$. We define $g_{t_1,t_2}(\boldsymbol{x}_k,j,\tilde{\boldsymbol{n}}_{j,l})$ as (cf. (10))

$$g_{t_1,t_2}(\boldsymbol{x}_k,j,\tilde{\boldsymbol{n}}_{j,l}) \triangleq \frac{P_j^{\mathrm{TX}}}{\sigma^2}\frac{\partial H_{j,k}^{\mathrm{LOS}}(\boldsymbol{x}_k,\tilde{\boldsymbol{n}}_{j,l})}{\partial x_{k,t_1}} \times \frac{\partial H_{j,k}^{\mathrm{LOS}}(\boldsymbol{x}_k,\tilde{\boldsymbol{n}}_{j,l})}{\partial x_{k,t_2}}\mathbb{1}_{\{(\boldsymbol{x}_k-\boldsymbol{l}_j)^T\tilde{\boldsymbol{n}}_{j,l}>0,\,(\boldsymbol{l}_j-\boldsymbol{x}_k)^T\bar{\boldsymbol{n}}_k>0\}} \quad (14)$$

and the vector of all possible $g_{t_1,t_2}(\boldsymbol{x}_k,j,\tilde{\boldsymbol{n}}_{j,l})$ values as

$$\boldsymbol{g}_{t_1,t_2}(\boldsymbol{x}_k) = \big[g_{t_1,t_2}(\boldsymbol{x}_k,1,\tilde{\boldsymbol{n}}_{1,1}),\ldots,g_{t_1,t_2}(\boldsymbol{x}_k,1,\tilde{\boldsymbol{n}}_{1,|\mathcal{N}_1|}), g_{t_1,t_2}(\boldsymbol{x}_k,2,\tilde{\boldsymbol{n}}_{2,1}),\ldots,g_{t_1,t_2}(\boldsymbol{x}_k,2,\tilde{\boldsymbol{n}}_{2,|\mathcal{N}_2|}),\ldots, g_{t_1,t_2}(\boldsymbol{x}_k,N_\mathrm{L},\tilde{\boldsymbol{n}}_{N_\mathrm{L},1}),\ldots,g_{t_1,t_2}(\boldsymbol{x}_k,N_\mathrm{L},\tilde{\boldsymbol{n}}_{N_\mathrm{L},|\mathcal{N}_{N_\mathrm{L}}|})\big]^T. \quad (15)$$

Next, we define a binary *selection vector* $\boldsymbol{z} = \left[\boldsymbol{z}_1^T\ldots\boldsymbol{z}_{N_\mathrm{L}}^T\right]^T$ with N_I ones, where each element $\boldsymbol{z}_j$ is an $|\mathcal{N}_j|$-dimensional binary column vector. In particular, each non-zero (unit) element of $\boldsymbol{z}$ determines which LED is selected and which orientation vector is utilized in each of the N_I time intervals. That is, for each $j\in\{1,\ldots,N_\mathrm{L}\}$,

$$z_{j,l} = \begin{cases}1, & \text{if } j\text{th LED with orientation } \tilde{\boldsymbol{n}}_{j,l} \text{ is selected}\\ 0, & \text{otherwise}\end{cases} \quad (16)$$

where $l\in\{1,\ldots,|\mathcal{N}_j|\}$ and $\boldsymbol{z}_j=[z_{j,1},\ldots,z_{j,|\mathcal{N}_j|}]^T$.

According to the definitions in (14)–(16), we can express the FIM in (10) for the discrete case as

$$[\mathbf{I}_k(\boldsymbol{z})]_{t_1,t_2} = \sum_{l=1}^{N_\mathrm{T}} z_l\,[\boldsymbol{g}_{t_1,t_2}(\boldsymbol{x}_k)]_l = \boldsymbol{z}^T\boldsymbol{g}_{t_1,t_2}(\boldsymbol{x}_k) \quad (17)$$

for $t_1,t_2\in\{1,2,3\}$, where $[\boldsymbol{g}_{t_1,t_2}(\boldsymbol{x}_k)]_l$ denotes the lth element of $\boldsymbol{g}_{t_1,t_2}(\boldsymbol{x}_k)$ in (15) and $N_\mathrm{T}\triangleq\sum_{j=1}^{N_\mathrm{L}}|\mathcal{N}_j|$.

Remark 2: When each LED transmitter can have only finitely many orientation vectors, the FIM in (10) corresponding to a strategy denoted by $\{s(i),\boldsymbol{n}_{s(i)}^i\}_{i=1}^{N_\mathrm{I}}$ can always be achieved by the FIM in (17) by appropriately defining the sets in (13) and the selection vector $\boldsymbol{z}$ (see (14)–(16)). For example, if an LED transmitter is employed with the same orientation vector in multiple time intervals by the strategy $\{s(i),\boldsymbol{n}_{s(i)}^i\}_{i=1}^{N_\mathrm{I}}$, the sets in (13) can be defined to have repetitions of the same orientation vector so that the FIM of that strategy can be achieved by (17).□

Based on the FIM in (17), the CRLB for the VLC receiver position $\boldsymbol{x}_k$ can be stated as

$$\mathrm{CRLB}_k(\boldsymbol{z}) \triangleq \operatorname{trace}\left\{\mathbf{I}_k^{-1}(\boldsymbol{z})\right\} = \operatorname{trace}\left\{\begin{bmatrix}\boldsymbol{z}^T\boldsymbol{g}_{1,1}(\boldsymbol{x}_k) & \boldsymbol{z}^T\boldsymbol{g}_{1,2}(\boldsymbol{x}_k) & \boldsymbol{z}^T\boldsymbol{g}_{1,3}(\boldsymbol{x}_k)\\ \boldsymbol{z}^T\boldsymbol{g}_{2,1}(\boldsymbol{x}_k) & \boldsymbol{z}^T\boldsymbol{g}_{2,2}(\boldsymbol{x}_k) & \boldsymbol{z}^T\boldsymbol{g}_{2,3}(\boldsymbol{x}_k)\\ \boldsymbol{z}^T\boldsymbol{g}_{3,1}(\boldsymbol{x}_k) & \boldsymbol{z}^T\boldsymbol{g}_{3,2}(\boldsymbol{x}_k) & \boldsymbol{z}^T\boldsymbol{g}_{3,3}(\boldsymbol{x}_k)\end{bmatrix}^{-1}\right\} \quad (18)$$

Then, the optimal LED selection and orientation adaptation problem can be formulated as the following selection problem (cf. (1)–(3)):

$$\underset{\boldsymbol{z}}{\text{minimize}} \sum_{k=1}^{N_\mathrm{U}} w_k\mathrm{CRLB}_k(\boldsymbol{z}) \quad (19)$$

$$\text{subject to } \mathbf{1}^T\boldsymbol{z}=N_\mathrm{I} \quad (20)$$

$$z_l\in\{0,1\},\ l=1,\ldots,N_\mathrm{T} \quad (21)$$

Since the problem in (19)–(21) has integer constraints, it does not lend itself to low-complexity solutions. Therefore, our approach is to relax the constraints in (21) as follows [52], [53]:

$$z_l\in[0,1],\ l=1,\ldots,N_\mathrm{T} \quad (22)$$

After this relaxation, the problem in (19)–(21) turns into a convex problem due to the following result.

Lemma 1: The objective function in (19) is a convex and non-increasing function of $\boldsymbol{z}$ for all $\boldsymbol{z}\succeq\mathbf{0}$.

Proof: Since $w_k\geq 0$ for all $k\in\{1,\ldots,N_\mathrm{U}\}$, it is sufficient to prove that $\mathrm{CRLB}_k(\boldsymbol{z})$ in (19) is a convex and non-increasing function of $\boldsymbol{z}$ for any k. For convexity, it is first noted that $\operatorname{trace}\{\mathbf{X}^{-1}\}$ is a convex function of $\mathbf{X}$ for any positive semidefinite matrix $\mathbf{X}$ [53]. Therefore, since $\mathbf{I}_k(\boldsymbol{z})$ specified in (18) is a linear function of $\boldsymbol{z}$, $\operatorname{trace}\left\{\mathbf{I}_k^{-1}(\boldsymbol{z})\right\}$, which is equal to $\mathrm{CRLB}_k(\boldsymbol{z})$, becomes a convex function of $\boldsymbol{z}$. For the non-increasing property, it is first noted that $\operatorname{trace}\{\mathbf{X}^{-1}\}$ is non-increasing with respect to $\mathbf{X}$; that is, if $\mathbf{X}'\succeq\mathbf{X}''$, then $\operatorname{trace}\{(\mathbf{X}')^{-1}\}\leq\operatorname{trace}\{(\mathbf{X}'')^{-1}\}$, where $\mathbf{X}'\succeq\mathbf{X}''$ means that $\mathbf{X}'-\mathbf{X}''$ is positive semidefinite. Hence, it is sufficient to show that $\boldsymbol{z}'\succeq\boldsymbol{z}''$ implies $\mathbf{I}_k(\boldsymbol{z}')\succeq\mathbf{I}_k(\boldsymbol{z}'')$, where $\boldsymbol{z}'\succeq\boldsymbol{z}''$ means that the lth element of $\boldsymbol{z}'$ is larger than or equal to the lth element of $\boldsymbol{z}''$ for each l. To show this, we define another vector $\tilde{\boldsymbol{z}}\triangleq\boldsymbol{z}'-\boldsymbol{z}''$. Clearly, $\tilde{\boldsymbol{z}}\succeq\mathbf{0}$. Also, we can write $\mathbf{I}_k(\tilde{\boldsymbol{z}})=\mathbf{I}_k(\boldsymbol{z}')-\mathbf{I}_k(\boldsymbol{z}'')$ from the linearity of $\mathbf{I}_k(\boldsymbol{z})$ with respect to $\boldsymbol{z}$. It is known that $\mathbf{I}_k(\tilde{\boldsymbol{z}})\succeq\mathbf{0}$ since $\tilde{\boldsymbol{z}}\succeq\mathbf{0}$. Then, $\mathbf{I}_k(\boldsymbol{z}')-\mathbf{I}_k(\boldsymbol{z}'')\succeq 0$; hence, $\mathbf{I}_k(\boldsymbol{z}')\succeq\mathbf{I}_k(\boldsymbol{z}'')$. ■

It follows from Lemma 1 that the relaxed version of the problem in (19)–(21) becomes a convex optimization problem, which is stated as

$$\underset{\boldsymbol{z}}{\text{minimize}} \sum_{k=1}^{N_\text{U}} w_k \text{CRLB}_k(\boldsymbol{z}) \tag{23}$$

$$\text{subject to} \quad \mathbf{1}^T \boldsymbol{z} = N_\text{I} \tag{24}$$

$$z_l \in [0,1],\ l = 1, \ldots, N_\text{T} \tag{25}$$

In addition, the non-increasing property in Lemma 1 implies that it is an optimal approach to send a signal in each time interval instead of having silent periods in some of the N_I intervals.

Based on the relaxed problem in (23)–(25), we propose the following algorithm (Algorithm 1) for LED selection and orientation adaptation:

Algorithm 1 Proposed Swap Algorithm to Find the Optimal LED Selection and Orientation Adaptation Strategy

```
Result: z^swp, CRLB_min
Find z^rel by solving (23)–(25);
Obtain z^lar by setting the largest N_I elements of z^rel
  to one and the others to zero;
Define CRLB_min = Σ_{k=1}^{N_U} w_k CRLB_k(z^lar);
for j = 1, ..., N_I do
    for i = 1, ..., N_swp do
        Obtain z* by replacing jth nonzero element in
          z^lar with the orientation corresponding to ith
          largest value in z^rel;
        CRLB = Σ_{k=1}^{N_U} w_k CRLB_k(z*);
        if CRLB < CRLB_min then
            CRLB_min = CRLB;
            z^swp = z*;
        end
    end
end
```

Remark 3: It is important to emphasize that the proposed LED selection and orientation adaptation strategy does not depend on the noise variance parameter σ^2 as it only scales the FIM (hence, CRLB), which can be noted from (10) or (14).□

Remark 4: The first step of the proposed strategy, (23)–(25), can be solved with the interior-point method, which runs in polynomial time, $\mathcal{O}(N_\text{T}^3)$, in the worst case (and much faster in practice). The remaining steps include the evaluation of the CRLB expression given in (18) for $N_\text{swp} \times N_\text{I}$ times, which has linear time complexity. Therefore, the complexity of our approach is $\mathcal{O}(N_\text{T}^3)$, which is significantly lower than that of multiple $2N_\text{L}$-dimensional searches required to solve the original problem in (1)–(3).□

Remark 5: The adaptation of the orientation vector of the photo-detector at the VLC receiver can also be incorporated into the proposed approach. If the orientation vectors, $\bar{\boldsymbol{n}}_k$, of the VLC receiver can take N_P possible values in each time interval, then the size of the selection vector $\boldsymbol{z}$ can be increased from N_T to $N_\text{T}N_\text{P}$. In that case, selecting an element of $\boldsymbol{z}$ specifies not only the selected LED and its orientation but also the orientation of the photo-detector at the VLC receiver. Hence, the proposed approach can be applied in this manner for joint adaptation of the orientations of the LED transmitters and the VLC receiver.□

IV. Special Case: A Distinct LED in Each Interval

For comparison purposes, we also consider a special case of the proposed formulation under the following assumptions:

- $N_\text{I} = N_\text{L}$.
- Each LED transmitter is employed in one of the intervals.

In this special case, the problem in (1)–(3) reduces to

$$\underset{\{\boldsymbol{n}_i\}_{i=1}^{N_\text{L}}}{\text{minimize}} \sum_{k=1}^{N_\text{U}} w_k \text{CRLB}_k \left(\{i, \boldsymbol{n}_i\}_{i=1}^{N_\text{L}}\right) \tag{26}$$

$$\text{subject to} \quad \|\boldsymbol{n}_i\| = 1,\ i = 1, \ldots, N_\text{L} \tag{27}$$

where $\boldsymbol{n}_i$ is the orientation vector of the ith LED transmitter, which is employed during the ith time interval. Since there is no need to perform selection in this special case, $\boldsymbol{n}_i$ is used instead of $\boldsymbol{n}_i^i$ (c.f. (1)) for a more compact notation.

For this case, the problem in (19)–(21) can be modified as

$$\underset{\boldsymbol{z}}{\text{minimize}} \sum_{k=1}^{N_\text{U}} w_k \text{CRLB}_k(\boldsymbol{z}) \tag{28}$$

$$\text{subject to} \quad \boldsymbol{e}_j^T \boldsymbol{z} = 1,\ j = 1, \ldots, N_\text{L} \tag{29}$$

$$z_l \in \{0,1\},\ l = 1, \ldots, N_\text{T} \tag{30}$$

where $\boldsymbol{e}_j$ is an $N_\text{T}-$dimensional binary column vector with its ℓth element being given by

$$[\boldsymbol{e}_j]_\ell = \begin{cases} 1, & \text{if } \ell \in \left\{\sum_{i=1}^{j-1} |\mathcal{N}_i| + 1, \ldots, \sum_{i=1}^{j} |\mathcal{N}_i|\right\} \\ 0, & \text{otherwise} \end{cases}. \tag{31}$$

The constraint in (29) enforces that each LED is used in exactly one of the intervals (cf. (20)).

For the problem in (28)–(30), similar steps to those in Section III can be performed by first replacing (30) with (22), and obtaining the relaxed solution denoted by $\tilde{\boldsymbol{z}}^\text{rel}$ via convex optimization. Then, the selection vector is obtained by setting the largest element in each of the N_L blocks of the relaxed solution $\tilde{\boldsymbol{z}}^\text{rel}$ to one and the others to zero, where the ith block of $\tilde{\boldsymbol{z}}^\text{rel}$ consists of $|\mathcal{N}_i|$ elements for $i = 1, \ldots, N_\text{L}$ (see (29) and (31)). The resulting selection vector for the special case is denoted by $\tilde{\boldsymbol{z}}^\text{lar}$. We can again employ the swap algorithm as in [52] and [54] and obtain an updated solution denoted by $\tilde{\boldsymbol{z}}^\text{swp}$.

As will be illustrated in the numerical examples, the general formulation in (1)–(3) (or, (19)–(21)) can lead to higher localization accuracy than the special case in (26)–(27) (or, (28)–(30)) since employing one LED with multiple orientations can sometimes provide considerably higher position related information than using multiple LEDs over the same time duration. On the other hand, the special case can outperform the conventional approaches in which all the LEDs have the same orientation (e.g., perpendicular to the ceiling) [14], [43].

V. Extension: Joint LED Selection and Power and Orientation Adaptation

In this section, we also consider the power allocation problem under a total power constraint together with the LED selection and orientation adaptation. Therefore, $P^{\rm TX}_{1,s(1)},\ldots,P^{\rm TX}_{N_{\rm I},s(N_{\rm I})}$ are regarded as additional optimization parameters, where $P^{\rm TX}_{i,s(i)}$ denotes the power parameter of the $s(i)$th LED transmitter during the time interval i. Accordingly, we extend the problem given in (1)–(3) as follows:

$$\underset{\left\{s(i),\boldsymbol{n}^i_{s(i)},P^{\rm TX}_{i,s(i)}\right\}_{i=1}^{N_{\rm I}}}{\text{minimize}} \sum_{k=1}^{N_{\rm U}} w_k {\rm CRLB}_k\left(\left\{s(i),\boldsymbol{n}^i_{s(i)},P^{\rm TX}_{i,s(i)}\right\}_{i=1}^{N_{\rm I}}\right) \tag{32}$$

$$\text{subject to}\quad s(i)\in\{1,\ldots,N_{\rm L}\},\ i=1,\ldots,N_{\rm I} \tag{33}$$

$$\left\|\boldsymbol{n}^i_{s(i)}\right\|=1,\ i=1,\ldots,N_{\rm I} \tag{34}$$

$$\sum_{i=1}^{N_{\rm I}} P^{\rm TX}_{i,s(i)}\le P_\Sigma \tag{35}$$

$$P^{\rm TX}_{i,s(i)}\ge 0,\ i=1,\ldots,N_{\rm I}, \tag{36}$$

where $P_\Sigma>0$ specifies the total power constraint, which is used to limit the total energy consumption of the VLP system.

Since the optimization problem in (32)–(36) corresponds to a high-dimensional non-convex problem, its direct/exhaustive solution is impractical. Therefore, as in Section III, we discretize the orientation vectors of the LEDs by updating the definitions of $g_{t_1,t_2}(\boldsymbol{x}_k,j,\tilde{\boldsymbol{n}}_{j,l})$ in (14) and $\boldsymbol{g}_{t_1,t_2}(\boldsymbol{x}_k)$ in (15) as

$$\hat{g}_{t_1,t_2}(\boldsymbol{x}_k,j,\tilde{\boldsymbol{n}}_{j,l})\triangleq\frac{1}{\sigma^2}\frac{\partial H^{\rm LOS}_{j,k}(\boldsymbol{x}_k,\tilde{\boldsymbol{n}}_{j,l})}{\partial x_{k,t_1}} \times\frac{\partial H^{\rm LOS}_{j,k}(\boldsymbol{x}_k,\tilde{\boldsymbol{n}}_{j,l})}{\partial x_{k,t_2}}\mathbb{1}_{\{(\boldsymbol{x}_k-\boldsymbol{l}_j)^T\tilde{\boldsymbol{n}}_{j,l}>0,\,(\boldsymbol{l}_j-\boldsymbol{x}_k)^T\bar{\boldsymbol{n}}_k>0\}} \tag{37}$$

and

$$\hat{\boldsymbol{g}}_{t_1,t_2}(\boldsymbol{x}_k)=\big[\hat{g}_{t_1,t_2}(\boldsymbol{x}_k,1,\tilde{\boldsymbol{n}}_{1,1}),\ldots,\hat{g}_{t_1,t_2}(\boldsymbol{x}_k,1,\tilde{\boldsymbol{n}}_{1,|\mathcal{N}_1|}), \hat{g}_{t_1,t_2}(\boldsymbol{x}_k,2,\tilde{\boldsymbol{n}}_{2,1}),\ldots,\hat{g}_{t_1,t_2}(\boldsymbol{x}_k,2,\tilde{\boldsymbol{n}}_{2,|\mathcal{N}_2|}),\ldots, \hat{g}_{t_1,t_2}(\boldsymbol{x}_k,N_{\rm L},\tilde{\boldsymbol{n}}_{N_{\rm L},1}),\ldots,\hat{g}_{t_1,t_2}(\boldsymbol{x}_k,N_{\rm L},\tilde{\boldsymbol{n}}_{N_{\rm L},|\mathcal{N}_{N_{\rm L}}|})\big]^T \tag{38}$$

and defining the power allocation vector $\boldsymbol{p}=\left[\boldsymbol{p}_1^T\ldots\boldsymbol{p}_{N_{\rm L}}^T\right]^T$, where each element $\boldsymbol{p}_j$ is an $|\mathcal{N}_j|$-dimensional column vector corresponding to the power parameters of LED j. That is, for each $j\in\{1,\ldots,N_{\rm L}\}$, $\boldsymbol{p}_j=[P^{\rm TX}_{j,1},\ldots,P^{\rm TX}_{j,|\mathcal{N}_j|}]^T$, where $P^{\rm TX}_{j,l}$ specifies the power allocated to the lth possible orientation of the jth LED transmitter for $l\in\{1,\ldots,|\mathcal{N}_j|\}$ (which is a non-negative real number, i.e., not discretized).

Similarly to (17), we can express the FIM in (10) for this case to include the power parameters as

$$[\mathbf{I}_k(\boldsymbol{z},\boldsymbol{p})]_{t_1,t_2}=\sum_{l=1}^{N_{\rm T}} z_l p_l\,[\hat{\boldsymbol{g}}_{t_1,t_2}(\boldsymbol{x}_k)]_l=(\boldsymbol{p}\odot\boldsymbol{z})^T\hat{\boldsymbol{g}}_{t_1,t_2}(\boldsymbol{x}_k) \tag{39}$$

for $t_1,t_2\in\{1,2,3\}$, where $[\hat{\boldsymbol{g}}_{t_1,t_2}(\boldsymbol{x}_k)]_l$ denotes the lth element of $\hat{\boldsymbol{g}}_{t_1,t_2}(\boldsymbol{x}_k)$ in (38). Based on the FIM in (39), the CRLB for the VLC receiver position $\boldsymbol{x}_k$ can be stated as

$${\rm CRLB}_k(\boldsymbol{z},\boldsymbol{p})\triangleq{\rm trace}\left\{\mathbf{I}_k^{-1}(\boldsymbol{z},\boldsymbol{p})\right\}. \tag{40}$$

Then, the joint LED selection and orientation and power adaptation problem can be formulated as

$$\underset{\boldsymbol{z},\boldsymbol{p}}{\text{minimize}}\ \sum_{k=1}^{N_{\rm U}} w_k{\rm CRLB}_k(\boldsymbol{z},\boldsymbol{p}) \tag{41}$$

$$\text{subject to}\quad \mathbf{1}^T\boldsymbol{z}=N_{\rm I} \tag{42}$$

$$z_l\in\{0,1\},\ l=1,\ldots,N_{\rm T} \tag{43}$$

$$\mathbf{1}^T\boldsymbol{p}\le P_\Sigma \tag{44}$$

$$\boldsymbol{p}\succeq\mathbf{0}. \tag{45}$$

We relax the constraints in (43) as in (22) to obtain the following relaxed problem:

$$\underset{\boldsymbol{z},\boldsymbol{p}}{\text{minimize}}\ \sum_{k=1}^{N_{\rm U}} w_k{\rm CRLB}_k(\boldsymbol{z},\boldsymbol{p}) \tag{46}$$

$$\text{subject to}\quad \mathbf{1}^T\boldsymbol{z}=N_{\rm I} \tag{47}$$

$$z_l\in[0,1],\ l=1,\ldots,N_{\rm T} \tag{48}$$

$$\mathbf{1}^T\boldsymbol{p}\le P_\Sigma \tag{49}$$

$$\boldsymbol{p}\succeq\mathbf{0}. \tag{50}$$

The problem given in (46)–(50) is a convex problem for given $\boldsymbol{z}$ or $\boldsymbol{p}$ due to the following result.

Lemma 2: The objective function in (46) is a convex and non-increasing function of $\boldsymbol{z}$ and $\boldsymbol{p}$ for all $\boldsymbol{z}\succeq\mathbf{0}$ and $\boldsymbol{p}\succeq\mathbf{0}$.

Proof: Since $w_k\ge 0$ for all $k\in\{1,\ldots,N_{\rm U}\}$, it is sufficient to prove that ${\rm CRLB}_k(\boldsymbol{z},\boldsymbol{p})$ in (46) is a convex and non-increasing function of $\boldsymbol{z}$ and $\boldsymbol{p}$ for any k. For convexity, it is first noted that ${\rm trace}\{\mathbf{X}^{-1}\}$ is a convex and non-increasing function of $\mathbf{X}$ for any positive semidefinite matrix $\mathbf{X}$ [53]. Therefore, it is sufficient to show that $\mathbf{I}_k(\boldsymbol{z},\boldsymbol{p})$ is a concave function of $\boldsymbol{z}$ and $\boldsymbol{p}$. From (39), it is noted that $\mathbf{I}_k(\boldsymbol{z},\boldsymbol{p})$ is linear with respect to $\boldsymbol{z}$ ($\boldsymbol{p}$) when $\boldsymbol{p}$ ($\boldsymbol{z}$) is fixed. Therefore, the objective function in (46) is convex for each of $\boldsymbol{z}$ and $\boldsymbol{p}$. The non-increasing property can be shown by defining $\boldsymbol{z}',\boldsymbol{z}'',\boldsymbol{p}'$ and $\boldsymbol{p}''$ where $\boldsymbol{z}'\succeq\boldsymbol{z}''$ and $\boldsymbol{p}'\succeq\boldsymbol{p}''$. Clearly, $\boldsymbol{z}'\odot\boldsymbol{p}'\succeq\boldsymbol{z}''\odot\boldsymbol{p}''$. Also, $\boldsymbol{I}_{\rm k}(\boldsymbol{z},\boldsymbol{p})$ is linear with respect to $\boldsymbol{z}\odot\boldsymbol{p}$. Therefore, similar to Lemma 1, ${\rm CRLB}_k(\boldsymbol{z},\boldsymbol{p})$ is a non-increasing function of $\boldsymbol{z}$ and $\boldsymbol{p}$. ■

Based on Lemma 2, the solution of (46)–(50) can be obtained in a low complexity manner via convex optimization tools by using alternating optimization. However, since all the elements of $\boldsymbol{z}$ are required to be integers, Algorithm 2 is proposed to optimize the power allocation following the application of the swap algorithm to determine $\boldsymbol{z}^{\rm swp}$. The algorithm first finds the solution, denoted by $\boldsymbol{z}^{\rm rel}$ and $\boldsymbol{p}^{\rm rel}$, to the problem in (46)–(50). It then performs a number of iterations, where in each iteration, a new solution $\boldsymbol{z}^*$ is generated from $\boldsymbol{z}^{\rm rel}$ using the swap algorithm mentioned in Section III. For this new $\boldsymbol{z}^*$, the corresponding optimal $\boldsymbol{p}^*$ is found by solving the following problem:

$$\underset{\boldsymbol{p}}{\text{minimize}}\ \sum_{k=1}^{N_{\rm U}} w_k{\rm CRLB}_k(\boldsymbol{z}^*,\boldsymbol{p}) \tag{51}$$

$$\text{subject to}\quad \mathbf{1}^T\boldsymbol{p}\le P_\Sigma \tag{52}$$

$$\boldsymbol{p}\succeq\mathbf{0}. \tag{53}$$

The power allocation problem in (51)–(53) for a given $\boldsymbol{z}^*$ is a convex problem, which can be seen from Lemma 2.

Algorithm 2 Proposed Algorithm to Find the Optimal LED Selection and Power and Orientation Adaptation Strategy

Result: $\boldsymbol{p}^{\text{opt}}, \boldsymbol{z}^{\text{opt}}, \text{CRLB}_{\min}$

Find $\boldsymbol{z}^{\text{rel}}, \boldsymbol{p}^{\text{rel}}$ by solving (46)–(50);
Obtain $\boldsymbol{z}^{\text{lar}}$ by setting the largest N_{I} elements of $\boldsymbol{z}^{\text{rel}}$ to one and the others to zero;
Define $\text{CRLB}_{\min} = \sum_{k=1}^{N_{\text{U}}} w_k \text{CRLB}_k(\boldsymbol{z}^{\text{lar}}, \boldsymbol{p}^{\text{rel}})$;
for $j = 1, \ldots, N_{\text{I}}$ **do**
  for $i = 1, \ldots, N_{\text{swp}}$ **do**
    Obtain $\boldsymbol{z}^*$ by replacing jth nonzero element in $\boldsymbol{z}^{\text{lar}}$ with the orientation corresponding to ith largest value in $\boldsymbol{z}^{\text{rel}}$;
    Find $\boldsymbol{p}^*$ from (54)–(56);
    $\text{CRLB} = \sum_{k=1}^{N_{\text{U}}} w_k \text{CRLB}_k(\boldsymbol{z}^*, \boldsymbol{p}^*)$;
    if $\text{CRLB} < \text{CRLB}_{\min}$ **then**
      $\text{CRLB}_{\min} = \text{CRLB}$;
      $(\boldsymbol{p}^{\text{opt}}, \boldsymbol{z}^{\text{opt}}) = (\boldsymbol{p}^*, \boldsymbol{z}^*)$;
    end
  end
end

The joint optimization problem in (46)–(50) can effectively be solved using the sequential quadratic programming (SQP) method during alternating optimization. In the MATLAB simulations, the SQP algorithm demonstrates faster convergence compared to the interior-point method. The computational complexity of the SQP algorithm can be approximated as $\mathcal{O}(N_{\text{T}}^3)$ in the worst case. At each iteration, the power optimization problem is solved with $\mathcal{O}(N_{\text{I}}^3)$ time complexity, since the solution $\boldsymbol{z}^*$ consists of N_{I} nonzero elements. Hence, the overall complexity of Algorithm 2 becomes $N_{\text{alt}} \times \mathcal{O}(N_{\text{T}}^3) + N_{\text{swp}} \times N_{\text{I}} \times \mathcal{O}(N_{\text{I}}^3)$, where N_{alt} is the number of iterations in alternating optimization, which is dominated by the term $\mathcal{O}(N_T^3)$ since $N_{\text{I}} < N_{\text{T}}$ in practical cases. This shows that the joint optimization can be performance without significantly increasing the time complexity compared to Algorithm 1.

VI. Numerical Results

A. System Setup

In this section, numerical results are presented to evaluate the performance of the proposed approaches. We consider a room with dimensions $8 \times 8 \times 5$ meters (width, depth, and height, respectively) and 4 LEDs (i.e., $N_{\text{L}} = 4$) placed at $\boldsymbol{l}_1 = [2, 2, 5]^T$ m, $\boldsymbol{l}_2 = [6, 2, 5]^T$ m, $\boldsymbol{l}_3 = [2, 6, 5]^T$ m, and $\boldsymbol{l}_4 = [6, 6, 5]^T$ m [13]. The transmit power parameters and the Lambertian orders of the LEDs are set, respectively, to $P_j^{\text{TX}} = 10\,\text{W}$ and $m_j = 1$ for all $j \in \{1, 2, 3, 4\}$. Also, the area of the photo-detector at the VLC receiver is $A = 1\,\text{cm}^2$.

The number of time intervals over which localization is performed is set to $N_{\text{I}} = 4$. For describing the prior statistical knowledge about the position of the VLC receiver, we generate two different $1 \times 1 \times 1$ m grids with 0.5 m step size between adjacent points in the grid. The VLC receiver may be at one of these points with equal probability, i.e., $w_k = 1/N_{\text{U}}$ for $k = 1, \ldots, N_{\text{U}}$, where $N_{\text{U}} = 27$. The center of the grid is taken as $[1, 1, 1]^T$ m for the first case (Case 1) and $[3, 4, 1]^T$ m for the second case (Case 2). In addition, the orientation vector of the VLC receiver is $\bar{\boldsymbol{n}}_k = [0, 0, 1]^T$ for all k in each case. The considered VLP system setup is shown in Fig. 2. For comparison purposes, we also consider the common approach with perpendicularly oriented LEDs, where each LED has the same orientation vector $\boldsymbol{n}_j = [0, 0, -1]^T$ for $j = 1, 2, 3, 4$. The prior probability distributions considered in Case 1 and Case 2 above can be used, for example, in a tracking application, where the center of the grid corresponds to the position estimate of the VLC receiver in the previous time step.

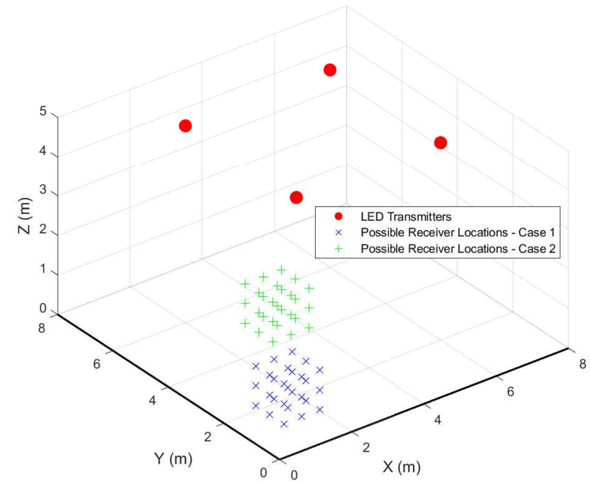

Fig. 2. VLP system configuration in the simulations. The center of grid is located at [1 1 1] m in Case 1 and at [3 4 1] m in Case 2.

To evaluate the performance of the proposed methods, we consider two different resolutions in determining the set of possible orientation vectors of the LED transmitters, i.e., sets $\mathcal{N}_j$ in (13). We first express the orientation vectors of the LED transmitters in $\mathcal{N}_j$ as $\tilde{\boldsymbol{n}}_{j,l} = [\sin\theta_l \cos\phi_l, \sin\theta_l \sin\phi_l, \cos\theta_l]^T$ for each $j \in \{1, \ldots, N_{\text{L}}\}$, where θ_l and ϕ_l denote the possible elevation and azimuth angles, respectively. Then, we introduce parameter Δ to uniformly sample the possible angles for the elevation and azimuth angles as follows: We sample the azimuth angle with 2Δ from 0^{o} to 360^{o} and the elevation angle with Δ from 180^{o} to 90^{o} (since the LEDs are on the ceiling of the room). Therefore, $(\theta_l, \phi_l) \in [180 : (-\Delta) : 90) \times [0 : 2\Delta : 360)$. In the simulations, $\Delta = 10\circ$ corresponds to the high resolution scenario and $\Delta = 30\circ$ to the low resolution scenario. For the swap algorithm in the proposed approach and its special case, $N_{\text{swp}} = 0.2|\mathcal{N}_j|$ is chosen, where $\mathcal{N}_j$ is as described above.

B. Evaluation of Proposed Approaches

First, we consider the LED selection and orientation adaptation approach proposed in Section III and its special case

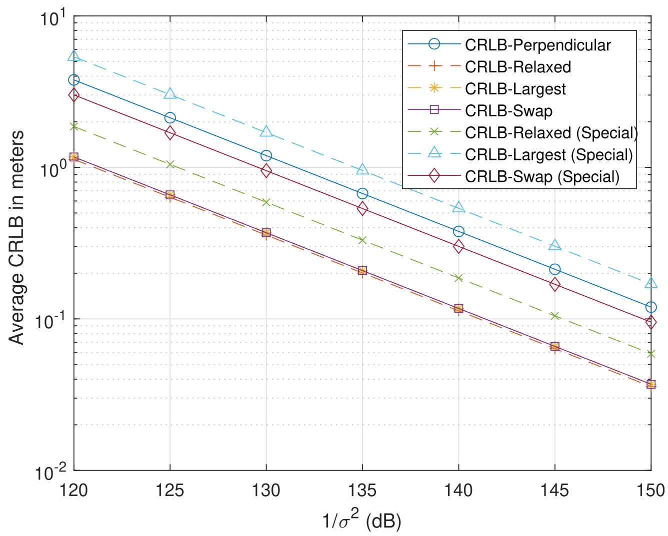

Fig. 3. Average CRLBs in meters in Case 1, when the receiver is close to the edge and $\Delta = 30\circ$.

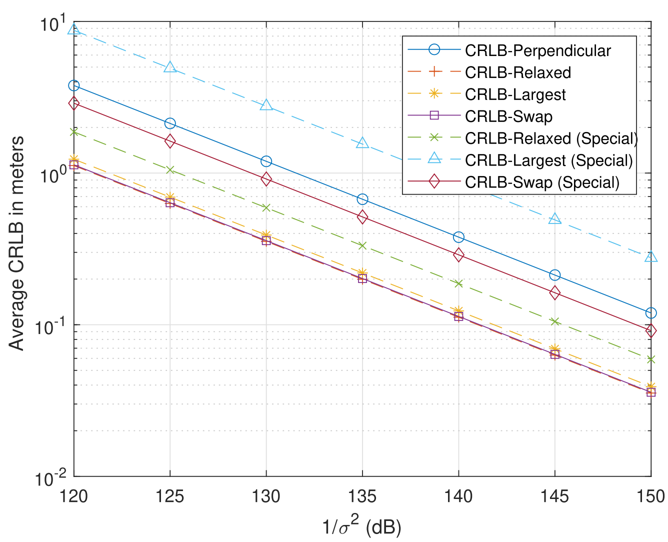

Fig. 4. Average CRLBs in meters in Case 1, when the receiver is close to the edge and $\Delta = 10\circ$.

TABLE I

LED SELECTIONS AND ORIENTATIONS FOR CASE 1, WHERE THE UPPER AND LOWER PARTS CORRESPOND TO THE PROPOSED APPROACH IN SECTION III AND ITS SPECIAL CASE IN SECTION IV, RESPECTIVELY

$\boldsymbol{z}^{\text{swp}}$, $\Delta = 30°$		$\boldsymbol{z}^{\text{swp}}$, $\Delta = 10°$	
LED	Orientation	LED	Orientation
1	[0.87 0 -0.50]	1	[0.81 0.30 -0.50]
1	[-0.43 0.75 -0.50]	1	[-0.75 0.63 -0.17]
1	[0.43 0.75 -0.50]	1	[0.15 0.85 -0.50]
1	[-0.43 -0.75 -0.50]	1	[-0.47 -0.81 -0.34]
$\tilde{\boldsymbol{z}}^{\text{swp}}$, $\Delta = 30°$		$\tilde{\boldsymbol{z}}^{\text{swp}}$, $\Delta = 10°$	
LED	Orientation	LED	Orientation
1	[-0.43 -0.75 -0.50]	1	[-0.67 -0.56 -0.50]
2	[-0.5 0 -0.87]	2	[-0.47 -0.17 -0.87]
3	[-0.25 -0.43 -0.87]	3	[-0.25 -0.43 -0.87]
4	[-0.25 -0.43 -0.87]	4	[-0.49 -0.41 -0.77]

TABLE II

LED SELECTIONS AND ORIENTATIONS FOR CASE 2, WHERE THE UPPER AND LOWER PARTS CORRESPOND TO THE PROPOSED APPROACH IN SECTION III AND ITS SPECIAL CASE IN SECTION IV, RESPECTIVELY

$\boldsymbol{z}^{\text{swp}}$, $\Delta = 30°$		$\boldsymbol{z}^{\text{swp}}$, $\Delta = 10°$	
LED	Orientation	LED	Orientation
1	[0.25 0.43 -0.87]	1	[0.17 0.30 -0.94]
2	[-0.25 0.43 -0.87]	2	[-0.38 -0.32 -0.87]
3	[0.25 -0.43 -0.87]	3	[0.17 -0.30 -0.94]
4	[-0.25 -0.43 -0.87]	4	[-0.38 -0.32 -0.87]
$\tilde{\boldsymbol{z}}^{\text{swp}}$, $\Delta = 30°$		$\tilde{\boldsymbol{z}}^{\text{swp}}$, $\Delta = 10°$	
LED	Orientation	LED	Orientation
1	[0.25 0.43 -0.87]	1	[0.17 0.30 -0.94]
2	[-0.25 0.43 -0.87]	2	[-0.38 -0.32 -0.87]
3	[0.25 -0.43 -0.87]	3	[0.17 -0.30 -0.94]
4	[-0.25 -0.43 -0.87]	4	[-0.38 -0.32 -0.87]

described in Section IV. In Fig. 3 and Fig. 4, the average CRLBs in meters achieved by the proposed solution $\boldsymbol{z}^{\text{swp}}$ ("CRLB–Swap"), the special case $\tilde{\boldsymbol{z}}^{\text{swp}}$ ("CRLB–Swap (Special)"), which enforces the use of each LED in only one interval, and the conventional perpendicular orientation approach ("CRLB–Perpendicular"), in which the LEDs are used in order and with perpendicular orientation, are plotted for Case 1 with respect to the noise variance σ^2. The average CRLBs are plotted in meters by taking the square-root of the average CRLB expressions in Sections III and IV. (The considered range of σ^2 values is compatible with those in the literature [43].) In addition, for illustrating the details of the algorithms, the CRLBs achieved by the relaxed problems ($\boldsymbol{z}^{\text{rel}}$ and $\tilde{\boldsymbol{z}}^{\text{rel}}$) and those achieved by setting the largest N_{I} elements of the relaxed solutions to one ($\boldsymbol{z}^{\text{lar}}$ and $\tilde{\boldsymbol{z}}^{\text{lar}}$) are presented in the figures with dashed lines. The results in Figs. 3 and 4 show that the proposed approach of LED selection and orientation adaptation significantly outperforms the special case and the perpendicular orientation approach when the receiver is near the edge of the room (Case 1). For example, when $1/\sigma^2 = 140\,$dB, the proposed approach ($\boldsymbol{z}^{\text{swp}}$), the special case ($\tilde{\boldsymbol{z}}^{\text{swp}}$), and the perpendicular orientation approach ($\boldsymbol{z}^{\text{per}}$) achieve average CRLBs of 0.12, 0.30, and 0.38 m, respectively. It is also noted that the proposed approach reaches a close value to that achieved by the relaxed solution, which provides a performance bound to the problem. Hence, the proposed convex relaxation approach combined with the swap algorithm does not cause a notable loss of optimality in this case. In addition, the change of resolution from $\Delta = 30\circ$ to $\Delta = 10\circ$ does not have a notable difference in the localization performance of the proposed approach, which is a desirable property for low complexity implementation.

In Table I, the solutions for the proposed approach and the special case are shown in Case 1 for both $\Delta = 10\circ$ and $\Delta = 30\circ$. It is noted that the proposed approach uses LED 1 (the closest LED to the possible receiver locations in Case 1) with certain orientations during all the four time intervals, and achieves lower CRLBs than the special case (as shown in Figs. 3 and 4), which uses each LED transmitter in only one of the intervals. Therefore, in this case, one LED provides more localization information than multiple LEDs by utilizing different orientations.

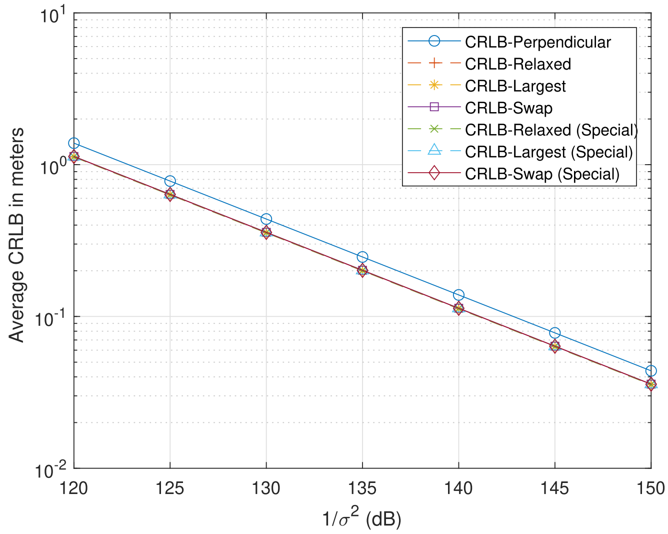

Fig. 5. Average CRLBs in meters in Case 2, when the receiver is close to the center for $\Delta = 30^\circ$.

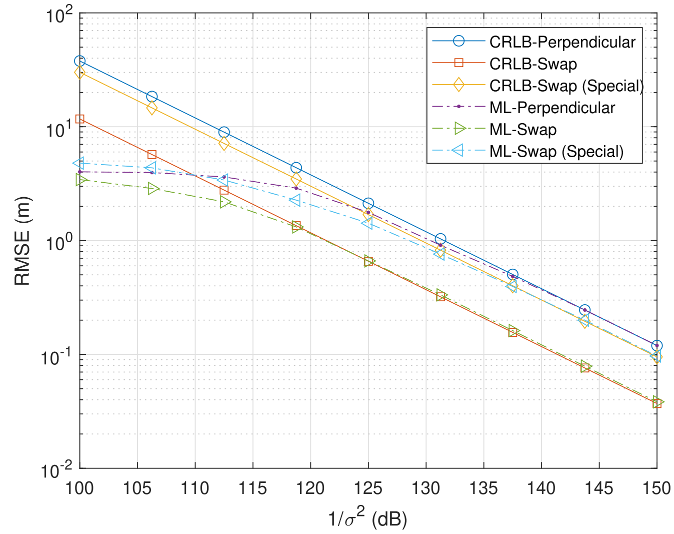

Fig. 7. RMSEs and average CRLBs in meters in Case 1, when the receiver is close to the edge and $\Delta = 30^\circ$.

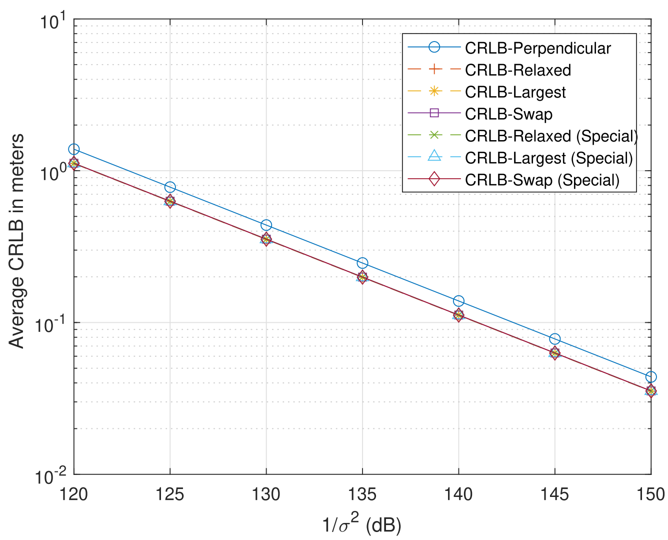

Fig. 6. Average CRLBs in meters in Case 2, when the receiver is close to the center for $\Delta = 10^\circ$.

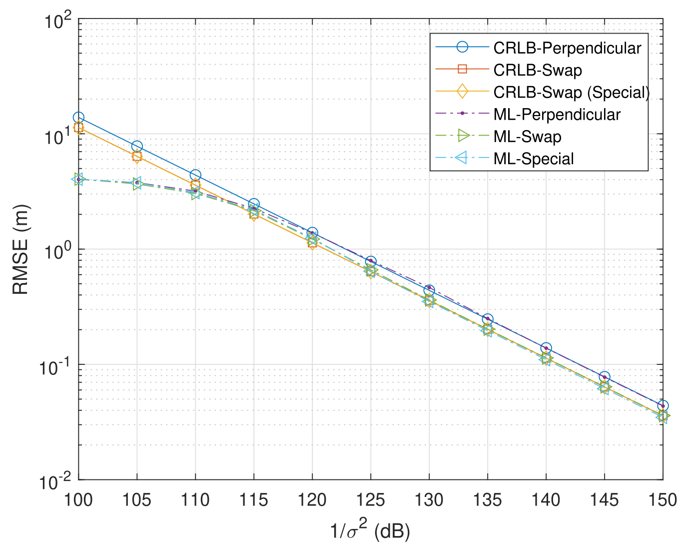

Fig. 8. RMSEs and average CRLBs in meters in Case 2, when the receiver is close to the center and $\Delta = 30^\circ$.

In Fig. 5 and Fig. 6, the CRLBs are plotted versus the noise variance for Case 2. In Case 2, the proposed approach improves the localization performance of the perpendicular orientation approach only by 2.53 cm at $1/\sigma^2 = 140$ dB for $\Delta = 30^\circ$. We also show in Table II that the solutions of the proposed method and the special case are the same. These observations are related to the fact that the possible VLC receiver positions are near the center of the room in Case 2 for which the optimal approach involves the use of all the LEDs with close to perpendicular orientations.

In Fig. 7 and Fig. 8, the RMSEs of the ML estimators (see (9)) and the CRLBs (in meters) are plotted for Case 1 and Case 2, respectively, for $\Delta = 30^\circ$. At each point, fifty trials are conducted. It can be seen that the RMSEs of the ML estimators converge to the CRLBs for all the methods at sufficiently low noise variances. Therefore, the proposed method not only reduces the CRLB but also improves the accuracy of the ML estimator, which is commonly used for localization. It is also noted that the RMSEs of the ML estimators are lower than the CRLBs for high noise variances, which is due to the fact that the ML estimator in (9) yields its estimate by performing a search for the VLC receiver position inside the room while the CRLB calculations do not assume any prior knowledge about the position of the VLC receiver.

Next, we focus on the joint LED selection and power and orientation adaptation approach proposed in Section V. Figs. 9 and 10 illustrate the average CRLBs achieved by the proposed swap approach, its special case, and the perpendicular configuration both in the absence and presence of power adaptation in Case 1 and Case 2, respectively. Namely, "CRLB-Joint" corresponds to the joint LED selection and orientation and power adaptation approach in Section V, and "CRLB-Joint (Special)" corresponds to its special case with

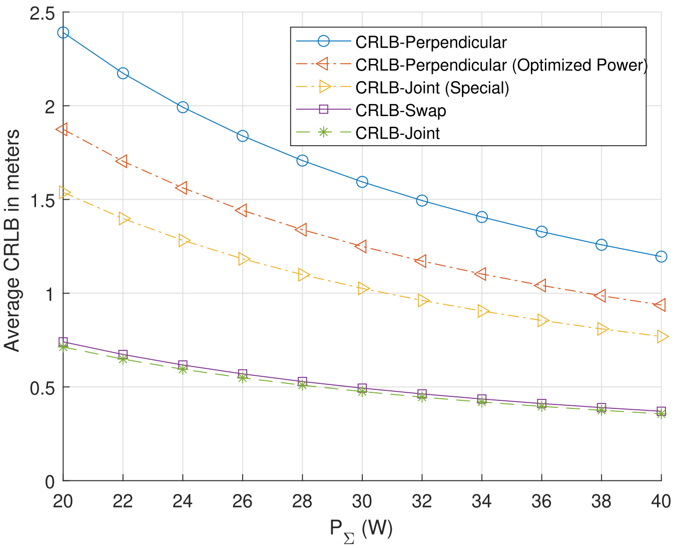

Fig. 9. Average CRLB (in meters) comparison of different strategies in Case 1, when the receiver is close to the edge, $\Delta = 30\circ$, and $1/\sigma^2 = 130\,\text{dB}$.

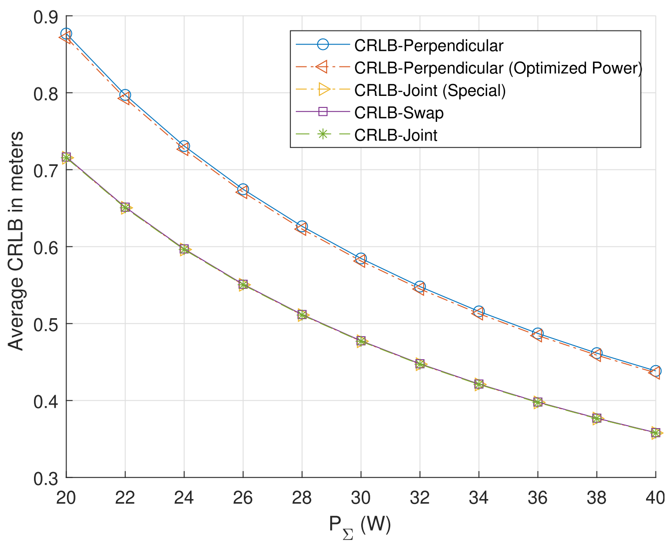

Fig. 10. Average CRLB (in meters) comparison of different strategies in Case 2, when the receiver is close to the center, $\Delta = 30\circ$, and $1/\sigma^2 = 130\,\text{dB}$.

TABLE III

LED Selections, Orientations, and Assigned Powers in Case 1 for the Proposed Approach in Section V, Where $P_\Sigma = 40\,\text{W}$

LED	Orientation	Power
1	[0.87 0 -0.50]	13.91
1	[-0.43 0.75 -0.50]	13.15
1	[0.43 0.75 -0.50]	1.71
1	[-0.43 -0.75 -0.50]	11.23

TABLE IV

LED Selections, Orientations, and Assigned Powers in Case 2 for the Proposed Approach in Section V, Where $P_\Sigma = 40\,\text{W}$

LED	Orientation	Power
1	[0.25 0.43 -0.87]	9.44
2	[-0.25 0.43 -0.87]	10.56
3	[0.25 -0.43 -0.87]	9.44
4	[-0.25 -0.43 -0.87]	10.56

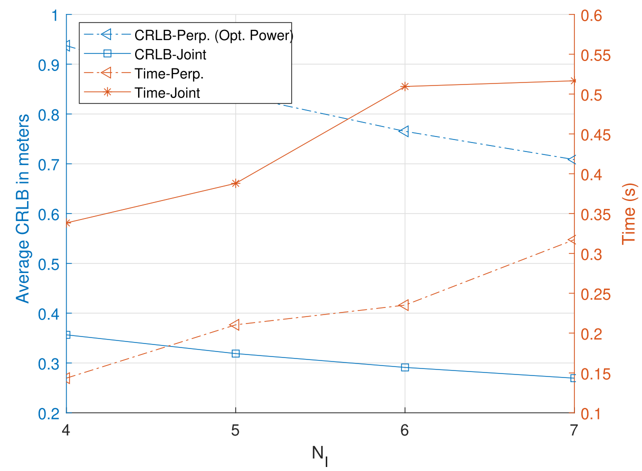

Fig. 11. Average CRLBs (in meters) and execution times of the proposed approach and the conventional approach (in which perpendicular LEDs are used in order and power optimization is performed) in Case 1, when the receiver is close to the edge, $\Delta = 30\circ$, and $1/\sigma^2 = 130\,\text{dB}$.

the use of each LED in one of the time intervals. It is observed that joint optimization can significantly reduce the average CRLBs for the special case of the proposed approach and for the conventional perpendicular configuration in Case 1. In addition, this reduction increases as the power constraint gets stricter. However, the swap approach gets only marginal benefits from power adaptation in this scenario (since optimization of LED selection and orientation adaptation achieves most of the improvements in this example). Moreover, when the receiver is close to the center (Case 2), power adaptation does not provide any notable benefits.

To provide more insights related to Figs. 9 and 10, Table III and Table IV show the optimized power allocation as well as the optimal LED selection and orientation adaptation based on the proposed approach in Case 1 and Case 2 when $P_\Sigma = 40\,\text{W}$. It can be seen that the differences among the assigned power levels is significantly larger in Case 1 compared to Case 2. This result indicates that power optimization can limit the power consumption for less informative orientations. Moreover, it is noted from Figs. 9 and 10 at $P_\Sigma = 40\,\text{W}$ that the difference in positioning accuracy between the two cases (Case 1 and Case 2) is minimal, namely, lower than 0.2%, when the proposed algorithm is used, whereas this difference increases to 53% and 63% for the perpendicular setup when the power is optimized and not optimized, respectively. Hence, a more homogeneous localization accuracy can be achieved over the environment via the proposed approach of LED selection, orientation, and power adaptation.

We also perform simulations for comparing the execution times of the proposed approach and the conventional approach in which perpendicular LEDs are used in order and power optimization is performed. Fig. 11 shows the effects of the number of time intervals N_I on the execution times and the average CRLBs (in meters) for both approaches in Case 1, where $\Delta = 30\circ$ and $1/\sigma^2 = 130\,\text{dB}$. Although the proposed approach requires approximately twice the time required by

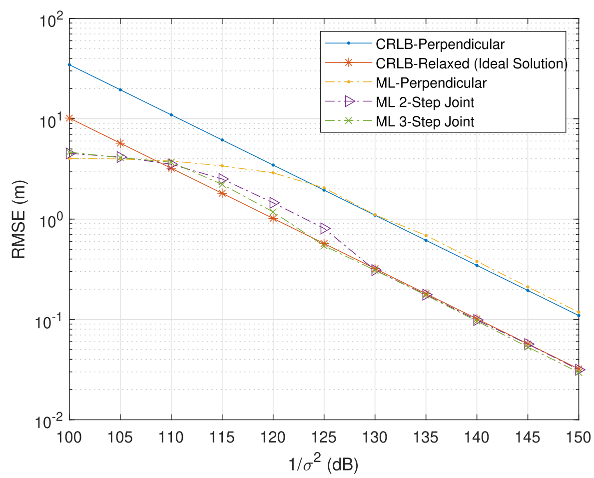

Fig. 12. RMSEs of the ML estimators in the multi-step algorithm together with the CRLBs (in meters) for the initial (perpendicular) configuration and for the ideal case of known VLC receiver position. In this case, the VLC receiver is located at $[1, 1, 1]^T$ m. and $\Delta = 30\circ$.

the conventional approach, it achieves a 62% reduction in the average CRLB (in meters). In addition, as stated before, the proposed approach achieves this improved localization performance with much lower computational complexity than the brute-force solution of (1)–(3), which has prohibitive complexity.

C. LED Selection and Orientation Adaptation in Absence of Prior Information on VLC Receiver Position

In this manuscript, a statistical uncertainty model is used for the unknown position of the VLC receiver. Namely, the uncertainty in the position of the VLC receiver is modeled by a prior probability distribution. In the absence of such prior information, LED selection and orientation adaptation can be performed iteratively with position estimation to achieve improved positioning and improved LED selection and orientation, which is similar to the multi-step algorithm in [46] in designing intelligent reflecting surface (IRS) parameters.

In this alternative approach, we first use a conventional setting for the LED selection and orientations, such as perpendicular setting (i.e., LEDs directly pointing downwards from the ceiling towards the floor) and using LEDs in order. Then, the VLC receiver performs ML estimation to determine its position and reports the position estimate to the localization network. Then, the LED selection and orientation optimization is performed assuming that the reported position is the true position of the VLC receiver; i.e., by setting $w_1 = 1$ for $\boldsymbol{x}_1 = \boldsymbol{x}_{\mathrm{ML}}$ and $w_i = 0$ for $i = 2, \ldots, N_{\mathrm{U}}$, where $\boldsymbol{x}_{\mathrm{ML}}$ denotes the ML position estimate. Then, based on this new LED selection and orientations, the VLC receiver performs another position estimate and reports it again. The results for this multi-step algorithm are shown in Fig. 12 by plotting the RMSEs of the ML estimators in the first three steps together with the CRLBs in meters for the initial configuration of LEDs (called "Perpendicular") and for the optimal configuration assuming that the position of the VLC receiver is known (called "Ideal Solution"). It can be seen that the multi-step approach converges to the CRLB for the ideal solution at sufficiently low noise variances. This result indicates that the proposed algorithm can be used even when there is no prior information about the position of the VLC receiver if the noise level is sufficiently low.

VII. Further Extensions

A. Incorporation of Illumination Constraints

We can consider two different application scenarios for the VLP system investigated in this manuscript.

- **Scenario 1:** In the first scenario, the VLP system is used in an environment where there are no requirements on illumination. For example, this would be the case in any indoor environment in the absence of people such as robot navigation in a dark factory, or machine/equipment tracking in an automated warehouse. In such cases, visible light or infrared signals (which have the same propagation characteristics as the visible light signals) can be used for positioning by considering the optimization of localization performance only, as considered in this study.
- **Scenario 2:** In the second scenario, the visible light system is also used for illumination. In such a case, the illumination constraints should be taken into account during the optimization of the VLP system. Therefore, the performance of localization and illumination are related to each other in this scenario.

Although the approaches in the previous section do not consider the illuminations constraints (i.e., focus on Scenario 1), the results can be extended to incorporate illumination constraints and to cover Scenario 2 as follows: As a measure of brightness, the illuminance $(\mathrm{lm/m^2}, \mathrm{lx})$ is used, which is defined as the luminous flux (lm) per unit area [55]. The horizontal illuminance at a given location $\boldsymbol{y}$ due to the jth LED transmitter during the ith time interval can be expressed as [56]

$$\mathcal{M}_j(\boldsymbol{y}, \boldsymbol{n}_j^i) = \frac{\sqrt{P_j^{\mathrm{TX}}}(m_j+1)\kappa_j E_j^{\mathrm{opt}} \left((\boldsymbol{y}-\boldsymbol{l}_j)^T \boldsymbol{n}_j^i\right)^{m_j} (l_{j,3}-y_3)}{2\pi \|\boldsymbol{y}-\boldsymbol{l}_j\|^{m_j+3}} \tag{54}$$

where $\boldsymbol{n}_j^i$ is the orientation vector of the jth LED during the ith time interval, $\boldsymbol{l}_j$ is the location of the jth LED transmitter, κ_j represents the luminous efficacy (lm/W) of the jth LED (the optical power to luminous flux conversion efficiency), E_j^{opt} is the optical power of the base signal used for transmission, and $l_{j,3}$ and y_3 denote the third components of $\boldsymbol{l}_j$ and $\boldsymbol{y}$, respectively. Assuming that LEDs are time multiplexed at a sufficiently high frequency (i.e., when the time intervals are sufficiently short), the perceived illuminance becomes the average of the illuminance provided by the employed LEDs over the time intervals such that

$$\mathcal{M}(\boldsymbol{y}) = \frac{1}{N_{\mathrm{I}}} \sum_{i=1}^{N_{\mathrm{I}}} \mathcal{M}_{s(i)}(\boldsymbol{y}, \boldsymbol{n}_{s(i)}^i)$$

where $\mathcal{M}(\boldsymbol{y})$ is the perceived illuminance at location $\boldsymbol{y}$ and $s(i)$ specifies the index of the LED transmitter selected for the ith time interval. If we consider L generic points $\boldsymbol{y}_1, \ldots, \boldsymbol{y}_L$ at which the illuminance constraints should be satisfied, then we can express the illumination constraints as

$$\mathcal{M}(\boldsymbol{y}_\ell) \geq \bar{\mathcal{M}}_\ell,\ \ell = 1, \ldots, L \tag{55}$$

where $\bar{\mathcal{M}}_\ell$ denotes the illuminance constraint defined for location $\boldsymbol{y}_\ell$.

In the discretization approach considered in Section III, the set of possible values for the orientation vector of the jth LED transmitter is represented by $\mathcal{N}_j = \{\tilde{\boldsymbol{n}}_{j,1}, \ldots, \tilde{\boldsymbol{n}}_{j,|\mathcal{N}_j|}\}$ for $j \in \{1, \ldots, N_{\mathrm{L}}\}$ as in (13). Then, we define the following vector considering all possible LEDs and all possible orientations as

$$\begin{aligned}\mathbf{m}(\boldsymbol{y}_\ell) = \big[&\mathcal{M}_1(\boldsymbol{y}_\ell, \tilde{\boldsymbol{n}}_{1,1}), \ldots, \mathcal{M}_1(\boldsymbol{y}_\ell, \tilde{\boldsymbol{n}}_{1,|\mathcal{N}_1|}), \ldots,\\ &\mathcal{M}_{N_{\mathrm{L}}}(\boldsymbol{y}_\ell, \tilde{\boldsymbol{n}}_{N_{\mathrm{L}},1}), \ldots, \mathcal{M}_{N_{\mathrm{L}}}(\boldsymbol{y}_\ell, \tilde{\boldsymbol{n}}_{N_{\mathrm{L}},|\mathcal{N}_{N_{\mathrm{L}}}|})\big]^T\end{aligned} \tag{56}$$

for $\ell \in \{1, \ldots, L\}$. Accordingly, the illumination constraints in (55) can be stated as

$$\mathbf{m}(\boldsymbol{y}_\ell)^T \boldsymbol{z} \geq \bar{\mathcal{M}}_\ell,\ \ell = 1, \ldots, L$$

where $\boldsymbol{z}$ is the $N_{\mathrm{T}}-$dimensional selection vector defined in Section III of the manuscript with $N_{\mathrm{T}} \triangleq \sum_{j=1}^{N_{\mathrm{L}}} |\mathcal{N}_j|$. Since these constraints are linear with respect to $\boldsymbol{z}$, adding them to the proposed convex problem in (23)–(25) does not change the convex structure of the problem.[6] In particular, the following optimization problem is considered instead of (23)–(25):

$$\begin{aligned}\underset{\boldsymbol{z}}{\text{minimize}}\ &\sum_{k=1}^{N_{\mathrm{U}}} w_k \mathrm{CRLB}_k(\boldsymbol{z})\\ \text{subject to}\ \ &\mathbf{1}^T \boldsymbol{z} = N_{\mathrm{I}}\\ &z_l \in [0,1],\ l = 1, \ldots, N_{\mathrm{T}}\\ &\mathbf{m}(\boldsymbol{y}_\ell)^T \boldsymbol{z} \geq \bar{\mathcal{M}}_\ell,\ \ell = 1, \ldots, L\end{aligned}$$

First, this convex problem is solved (assuming that it is feasible; i.e., that the illumination constraints are not too strict), and its solution is denoted by $\boldsymbol{z}^{\mathrm{rel}}$. Then, the largest N_{I} elements of $\boldsymbol{z}^{\mathrm{rel}}$ are set to one and the other elements are set to zero. The resulting vector is called $\boldsymbol{z}^{\mathrm{lar}}$. Next, a swap algorithm is performed similarly to Algorithm 1 by performing swaps between the nonzero elements of $\boldsymbol{z}^{\mathrm{lar}}$ and the orientations corresponding to ith largest value in $\boldsymbol{z}^{\mathrm{rel}}$ for $i = 1, \ldots, N_{\mathrm{swp}}$. However, unlike Algorithm 1, a feasibility check is performed for each candidate selection vector formed during the swap operations, and the one that is feasible *and* achieves the minimum objective (i.e., average CRLB) is selected as the current solution candidate. Overall, the proposed discretization and convex relaxation approach followed by the swap algorithm can also be applied by considering illumination constraints, as well.

[6]It is also possible to incorporate an average illumination constraint as in Section III.C.4 of [56] into the problem as another linear constraint.

B. Extension to the Case of Multiple Receivers

The approaches in this manuscript can directly be extended to cover the case of multiple VLC receivers (users). In that case, a weighted average of the average CRLBs of multiple receivers can be employed as the objective function. Let N_{B} denote the number of VLC receivers and $\boldsymbol{x}_k^{(b)}$ and $\bar{\boldsymbol{n}}_k^{(b)}$ represent, respectively, the position and the orientation vector of the bth user at its kth possible location, where $b \in \{1, \ldots, N_{\mathrm{B}}\}$ and $k \in \{1, \ldots, N_{\mathrm{U}}^{(b)}\}$, with $N_{\mathrm{U}}^{(b)}$ denoting the number of possible locations for the bth VLC receiver. Also, $w_k^{(b)}$ represents the probability that the bth VLC receiver is at position $\boldsymbol{x}_k^{(b)}$. We also introduce importance factors (weights) for different VLC receivers denoted by $\xi^{(1)}, \ldots, \xi^{(B)}$, which are non-negative coefficients. Then, we propose the following problem for LED selection and orientation adaptation for multiple VLC receivers (cf. (1)–(3)):

$$\begin{aligned}\underset{\{s(i), \boldsymbol{n}^i_{s(i)}\}_{i=1}^{N_{\mathrm{I}}}}{\text{minimize}}\ &\sum_{b=1}^{B} \xi^{(b)} \sum_{k=1}^{N_{\mathrm{U}}^{(b)}} w_k^{(b)} \mathrm{CRLB}_k^{(b)}\left(\left\{s(i), \boldsymbol{n}^i_{s(i)}\right\}_{i=1}^{N_{\mathrm{I}}}\right)\\ \text{subject to}\ \ &s(i) \in \{1, \ldots, N_{\mathrm{L}}\},\ i = 1, \ldots, N_{\mathrm{I}}\\ &\left\|\boldsymbol{n}^i_{s(i)}\right\| = 1,\ i = 1, \ldots, N_{\mathrm{I}}\end{aligned}$$

where the CRLB term denoted by $\mathrm{CRLB}_k^{(b)}\left(\left\{s(i), \boldsymbol{n}^i_{s(i)}\right\}_{i=1}^{N_{\mathrm{I}}}\right)$ can be obtained as in Section III by replacing $\boldsymbol{x}_k$, $\bar{\boldsymbol{n}}_k$ and A with $\boldsymbol{x}_k^{(b)}$, $\bar{\boldsymbol{n}}_k^{(b)}$ and $A^{(b)}$, respectively, with $A^{(b)}$ being the area of the photo-detector at the bth VLC receiver.

Since the structure of the problem is the same as that in (1)–(3), all the theoretical approaches apply to this problem, as well. For example, the problem in (19)–(21) turns into

$$\begin{aligned}\underset{\boldsymbol{z}}{\text{minimize}}\ &\sum_{b=1}^{B} \xi^{(b)} \sum_{k=1}^{N_{\mathrm{U}}} w_k^{(b)} \mathrm{CRLB}_k^{(b)}(\boldsymbol{z})\\ \text{subject to}\ \ &\mathbf{1}^T \boldsymbol{z} = N_{\mathrm{I}}\\ &z_l \in \{0,1\},\ l = 1, \ldots, N_{\mathrm{T}}\end{aligned}$$

which again becomes a convex problem after relaxation. Hence, the same algorithms can be applied.

VIII. Concluding Remark

We have proposed an algorithm for LED selection and orientation adaptation for VLP systems with the aim of minimizing the average CRLB on position estimation. By considering a finite set of possible orientation vectors for each LED transmitter, we have utilized a convex relaxation approach to develop a low-complexity algorithm. Numerical results have illustrated the effectiveness of the proposed approach in various scenarios.

We have also proposed an algorithm for joint LED selection and power and orientation adaptation to minimize the average CRLB. By extending our approach to a finite set of possible orientation vectors, we have added a power vector associated with the orientation vector for each LED transmitter. We have proved that the same relaxation approach can be used in this problem to obtain a new problem. Simulations have shown that joint optimization can be beneficial under strict power constraints and increase performance significantly compared to the case without power optimization, depending on the maximum power limitation and system settings.

An extension of this work can be performed by considering communication constraints in a multi-user VLC system. Another direction for future work may include the incorporation of intelligent reflecting surface (IRS) components to increase the positioning accuracy in both LOS and non-LOS scenarios. It is also important to investigate the LED selection and orientation (and power) adaptation problem when the orientation vector of the VLC receiver is unknown and the aim is to perform joint position and orientation estimation for the VLC receiver. Finally, the proposed approaches for LED selection and orientation and power adaptation can be evaluated via experiments considering real application scenarios. In this way, the real-time capabilities of the proposed approaches can be assessed, and suitable application scenarios (such as indoor robotic applications with service robots or warehouse/logistics robots) can be identified. In particular, the speed of implementing the proposed algorithms as well as the speed of orientation adjustment of LEDs (e.g., with the use of MEMS micromirrors to tilt the beam) are critical parameters for real-time applications.

REFERENCES

[1] B. Asilioglu and S. Gezici, "LED selection and orientation adaptation for indoor visible light positioning systems," in *Proc. IEEE Int. Symp. Pers., Indoor Mobile Radio Commun. (PIMRC)*, Sep. 2025, pp. 1–6.

[2] P. Dwivedy, V. Dixit, and A. Kumar, "A survey on visible light communication for 6G: Architecture, application and challenges," in *Proc. Int. Conf. Comput., Electron. Electr. Eng. Appl. (IC2E3)*, Jun. 2023, pp. 1–6.

[3] Y. Lu and X. Zheng, "6G: A survey on technologies, scenarios, challenges, and the related issues," *J. Ind. Inf. Integr.*, vol. 19, pp. 1–14, Sep. 2020.

[4] M. F. Keskin, A. D. Sezer, and S. Gezici, "Localization via visible light systems," *Proc. IEEE*, vol. 106, no. 6, pp. 1063–1088, Jun. 2018.

[5] J. Armstrong, Y. A. Sekercioglu, and A. Neild, "Visible light positioning: A roadmap for international standardization," *IEEE Commun. Mag.*, vol. 51, no. 12, pp. 68–73, Dec. 2013.

[6] Y. Zhuang et al., "A survey of positioning systems using visible LED lights," *IEEE Commun. Surveys Tuts.*, vol. 20, no. 3, pp. 1963–1988, 3rd Quart., 2018.

[7] H. Steendam, T. Q. Wang, and J. Armstrong, "Theoretical lower bound for indoor visible light positioning using received signal strength measurements and an aperture-based receiver," *J. Lightw. Technol.*, vol. 35, no. 2, pp. 309–319, Jan. 15, 2017.

[8] W. Zhang, M. I. S. Chowdhury, and M. Kavehrad, "Asynchronous indoor positioning system based on visible light communications," *Opt. Eng.*, vol. 53, no. 4, Apr. 2014, Art. no. 045105.

[9] M. Aminikashani, W. Gu, and M. Kavehrad, "Indoor positioning in high speed OFDM visible light communications," 2015, *arXiv:1505.01811*.

[10] W. Xu, J. Wang, H. Shen, H. Zhang, and X. You, "Indoor positioning for multiphotodiode device using visible-light communications," *IEEE Photon. J.*, vol. 8, no. 1, pp. 1–11, Feb. 2016.

[11] B. Zhou, V. Lau, Q. Chen, and Y. Cao, "Simultaneous positioning and orientating for visible light communications: Algorithm design and performance analysis," *IEEE Trans. Veh. Technol.*, vol. 67, no. 12, pp. 11790–11804, Dec. 2018.

[12] Y. Zhuang et al., "Visible light positioning and navigation using noise measurement and mitigation," *IEEE Trans. Veh. Technol.*, vol. 68, no. 11, pp. 11094–11106, Nov. 2019.

[13] M. F. Keskin, S. Gezici, and O. Arikan, "Direct and two-step positioning in visible light systems," *IEEE Trans. Commun.*, vol. 66, no. 1, pp. 239–254, Jan. 2018.

[14] T. Q. Wang, Y. A. Sekercioglu, A. Neild, and J. Armstrong, "Position accuracy of time-of-arrival based ranging using visible light with application in indoor localization systems," *J. Lightw. Technol.*, vol. 31, no. 20, pp. 3302–3308, Oct. 15, 2013.

[15] H. Steendam, T. Q. Wang, and J. Armstrong, "Cramer-Rao bound for AOA-based VLP with an aperture-based receiver," in *Proc. IEEE Int. Conf. Commun. (ICC)*, May 2017, pp. 1–6.

[16] A. Sahin, Y. S. Eroglu, I. Guvenc, N. Pala, and M. Yuksel, "Accuracy of AOA-based and RSS-based 3D localization for visible light communications," in *Proc. IEEE 82nd Veh. Technol. Conf. (VTC-Fall)*, Boston, MA, USA, Sep. 2015, pp. 1–5.

[17] T.-H. Do, J. Hwang, and M. Yoo, "TDoA based indoor visible light positioning systems," in *Proc. 5th Int. Conf. Ubiquitous Future Netw. (ICUFN)*, Jul. 2013, pp. 456–458.

[18] S.-H. Yang, H.-S. Kim, Y.-H. Son, and S.-K. Han, "Three-dimensional visible light indoor localization using AOA and RSS with multiple optical receivers," *J. Lightw. Technol.*, vol. 32, no. 14, pp. 2480–2485, Jul. 15, 2014.

[19] G. B. Prince and T. D. C. Little, "Latency constrained device positioning using a visible light communication two-phase received signal strength–angle of arrival algorithm," in *Proc. Int. Conf. Indoor Positioning Indoor Navigat. (IPIN)*, Oct. 2015, pp. 1–7.

[20] A. Sahin, Y. S. Eroglu, I. Guvenc, N. Pala, and M. Yuksel, "Hybrid 3-D localization for visible light communication systems," *J. Lightw. Technol.*, vol. 33, no. 22, pp. 4589–4599, Nov. 15, 2015.

[21] M. A. Arfaoui et al., "Invoking deep learning for joint estimation of indoor LiFi user position and orientation," *IEEE J. Sel. Areas Commun.*, vol. 39, no. 9, pp. 2890–2905, Sep. 2021.

[22] Y. Chen, W. Guan, J. Li, and H. Song, "Indoor real-time 3-D visible light positioning system using fingerprinting and extreme learning machine," *IEEE Access*, vol. 8, pp. 13875–13886, 2020.

[23] F. Alam, M. T. Chew, T. Wenge, and G. S. Gupta, "An accurate visible light positioning system using regenerated fingerprint database based on calibrated propagation model," *IEEE Trans. Instrum. Meas.*, vol. 68, no. 8, pp. 2714–2723, Aug. 2019.

[24] M. T. Van, N. Van Tuan, T. T. Son, H. Le-Minh, and A. Burton, "Weighted k-nearest neighbour model for indoor VLC positioning," *IET Commun.*, vol. 11, no. 6, pp. 864–871, Apr. 2017.

[25] H. H. Heqing Huang, A. Y. Aiying Yang, L. F. Lihui Feng, G. N. Guoqiang Ni, A. P. G.,and P. Guo, "Artificial neural-network-based visible light positioning algorithm with a diffuse optical channel," *Chin. Opt. Lett.*, vol. 15, no. 5, pp. 050601–50605, 2017.

[26] S. Aboagye, A. R. Ndjiongue, T. M. N. Ngatched, O. A. Dobre, and H. V. Poor, "RIS-assisted visible light communication systems: A tutorial," *IEEE Commun. Surveys Tuts.*, vol. 25, no. 1, pp. 251–288, 1st Quart., 2023.

[27] E. Tarhan, F. Kokdogan, and S. Gezici, "IRS aided visible light positioning with a single LED transmitter," *Digit. Signal Process.*, vol. 156, Jan. 2025, Art. no. 104799.

[28] S. S. Saab and K. K. Saab, "A positioning system for photodiode device using collocated LEDs," *IEEE Photon. J.*, vol. 8, no. 5, pp. 1–14, 2016.

[29] Z. Saghir and S. Aboagye, "Movable access point-aided integrated visible light communication and sensing networks," *IEEE Wireless Commun. Lett.*, vol. 14, no. 3, pp. 731–735, Mar. 2025.

[30] M. Le Tran and S. Kim, "Joint power allocation and orientation for uniform illuminance in indoor visible light communication," *Opt. Exp.*, vol. 27, no. 20, pp. 28575–28587, Sep. 2019.

[31] N. Chaudhary, O. I. Younus, L. N. Alves, Z. Ghassemlooy, S. Zvánovec, and H. L. Minh, "An indoor visible light positioning system using tilted LEDs with high accuracy," *Sensors*, vol. 21, no. 3, p. 920, 2021.

[32] F. Wu, N. Stevens, L. De Strycker, and F. Rottenberg, "Enhancing RSS-based visible light positioning by optimal calibration of LED tilt and gain," *IEEE Trans. Commun.*, vol. 73, no. 9, pp. 7771–7783, Sep. 2025.

[33] R. Liu, Z. Liang, K. Yang, and W. Li, "Machine learning based visible light indoor positioning with single-LED and single rotatable photo detector," *IEEE Photon. J.*, vol. 14, no. 3, pp. 1–11, Jun. 2022.

[34] H. Shi, C. Wang, and Y. Zhao, "Visible light positioning using a single LED and a single rotatable photodetector," *IEEE Photon. Technol. Lett.*, vol. 37, no. 18, pp. 1033–1036, Sep. 2025.

[35] J. M. Menéndez and H. Steendam, "Influence of the aperture-based receiver orientation on RSS-based VLP performance," in *Proc. Int. Conf. Indoor Positioning Indoor Navigat. (IPIN)*, Sep. 2017, pp. 1–7.

[36] N. Stevens and H. Steendam, “Influence of transmitter and receiver orientation on the channel gain for RSS ranging-based VLP,” in *Proc. 11th Int. Symp. Commun. Syst., Netw. Digit. Signal Process. (CSNDSP)*, Jul. 2018, pp. 1–5.
[37] A. Nuwanpriya, S.-W. Ho, and C. S. Chen, “Angle diversity receiver for indoor MIMO visible light communications,” in *Proc. IEEE Globecom Workshops (GC Wkshps)*, Dec. 2014, pp. 444–449.
[38] M. Le Tran and S. Kim, “Orientation-induced link-blocked receiver for MIMO visible light communication,” *Opt. Exp.*, vol. 28, no. 8, p. 12157, Apr. 2020.
[39] C. Chen, W.-D. Zhong, H. Yang, S. Zhang, and P. Du, “Reduction of SINR fluctuation in indoor multi-cell VLC systems using optimized angle diversity receiver,” *J. Lightw. Technol.*, vol. 36, no. 17, pp. 3603–3610, Sep. 2018.
[40] P. Cherntanomwong and W. Chantharasena, “Indoor localization system using visible light communication,” in *Proc. 7th Int. Conf. Inf. Technol. Electr. Eng. (ICITEE)*, Oct. 2015, pp. 480–483.
[41] Y. Hou, S. Xiao, H. Zheng, and W. Hu, “Multiple access scheme based on block encoding time division multiplexing in an indoor positioning system using visible light,” *J. Opt. Commun. Netw.*, vol. 7, no. 5, pp. 489–495, May 2015.
[42] H. V. Poor, *An Introduction To Signal Detection and Estimation*. Cham, Switzerland: Springer, 1994.
[43] X. Zhang, J. Duan, Y. Fu, and A. Shi, “Theoretical accuracy analysis of indoor visible light communication positioning system based on received signal strength indicator,” *J. Lightw. Technol.*, vol. 32, no. 21, pp. 4180–4186, Nov. 1, 2014.
[44] T. Komine and M. Nakagawa, “Fundamental analysis for visible-light communication system using LED lights,” *IEEE Trans. Consum. Electron.*, vol. 50, no. 1, pp. 100–107, Feb. 2004.
[45] E. Gonendik and S. Gezici, “Fundamental limits on RSS based range estimation in visible light positioning systems,” *IEEE Commun. Lett.*, vol. 19, no. 12, pp. 2138–2141, Dec. 2015.
[46] F. Kokdogan and S. Gezici, “Intelligent reflecting surfaces for visible light positioning based on received power measurements,” *IEEE Trans. Veh. Technol.*, vol. 73, no. 9, pp. 13108–13121, Sep. 2024.
[47] S. Shen, S. Li, and H. Steendam, “Simultaneous position and orientation estimation for visible light systems with multiple LEDs and multiple PDs,” *IEEE J. Sel. Areas Commun.*, vol. 38, no. 8, pp. 1866–1879, Aug. 2020.
[48] G. Kail, P. Maechler, N. Preyss, and A. Burg, “Robust asynchronous indoor localization using LED lighting,” in *Proc. IEEE Int. Conf. Acoust. Speech Signal Process. (ICASSP)*, Florence, Italy, May 2014, pp. 1866–1870.
[49] O. González, S. Rodríguez, R. Pérez-Jiménez, B. R. Mendoza, and A. Ayala, “Error analysis of the simulated impulse response on indoor wireless optical channels using a Monte Carlo-based ray-tracing algorithm,” *IEEE Trans. Commun.*, vol. 53, no. 1, pp. 124–130, Jan. 2005.
[50] A. M. Abdelhady, A. K. S. Salem, O. Amin, B. Shihada, and M.-S. Alouini, “Visible light communications via intelligent reflecting surfaces: Metasurfaces vs mirror arrays,” *IEEE Open J. Commun. Soc.*, vol. 2, pp. 1–20, 2021.
[51] J. M. Kahn and J. R. Barry, “Wireless infrared communications,” *Proc. IEEE*, vol. 85, no. 2, pp. 265–298, Feb. 1997.
[52] C. Ozturk and S. Gezici, “Eavesdropper and jammer selection in wireless source localization networks,” *IEEE Trans. Signal Process.*, vol. 69, pp. 4341–4356, 2021.
[53] S. Boyd and L. Vandenberghe, *Convex Optimization*. Cambridge, U.K.: Cambridge Univ. Press, 2004.
[54] S. Joshi and S. Boyd, “Sensor selection via convex optimization,” *IEEE Trans. Signal Process.*, vol. 57, no. 2, pp. 451–462, Feb. 2009.
[55] E. F. Schubert, *Light-Emitting Diodes*. Cambridge, U.K.: Cambridge Univ. Press, 2003.
[56] M. F. Keskin, A. D. Sezer, and S. Gezici, “Optimal and robust power allocation for visible light positioning systems under illumination constraints,” *IEEE Trans. Commun.*, vol. 67, no. 1, pp. 527–542, Jan. 2019.

Baran Asilioglu (Student Member, IEEE) received the B.S. degree from the Department of Electrical and Electronics Engineering, Bilkent University, Ankara, Türkiye, in 2024. He is currently pursuing the M.S. degree in the same department. His current research interests include visible light communications and localization systems.

Sinan Gezici (Fellow, IEEE) received the B.Sc. degree in electrical and electronics engineering from Bilkent University, Ankara, Türkiye, in 2001, and the Ph.D. degree in electrical engineering from Princeton University, Princeton, NJ, USA, in 2006. From 2006 to 2007, he was with the Mitsubishi Electric Research Laboratories, Cambridge, MA, USA. Since 2007, he has been with the Department of Electrical and Electronics Engineering, Bilkent University, where he is currently a Professor. Among his publications in these areas is the book *Ultra-Wideband Positioning Systems: Theoretical Limits, Ranging Algorithms, and Protocols* (Cambridge University Press, 2008). His research interests include detection and estimation theory, wireless communications, and localization systems. He has been an Associate Editor of IEEE TRANSACTIONS ON VEHICULAR TECHNOLOGY, IEEE TRANSACTIONS ON COMMUNICATIONS, IEEE WIRELESS COMMUNICATIONS LETTERS, and *Journal of Communications and Networks*.